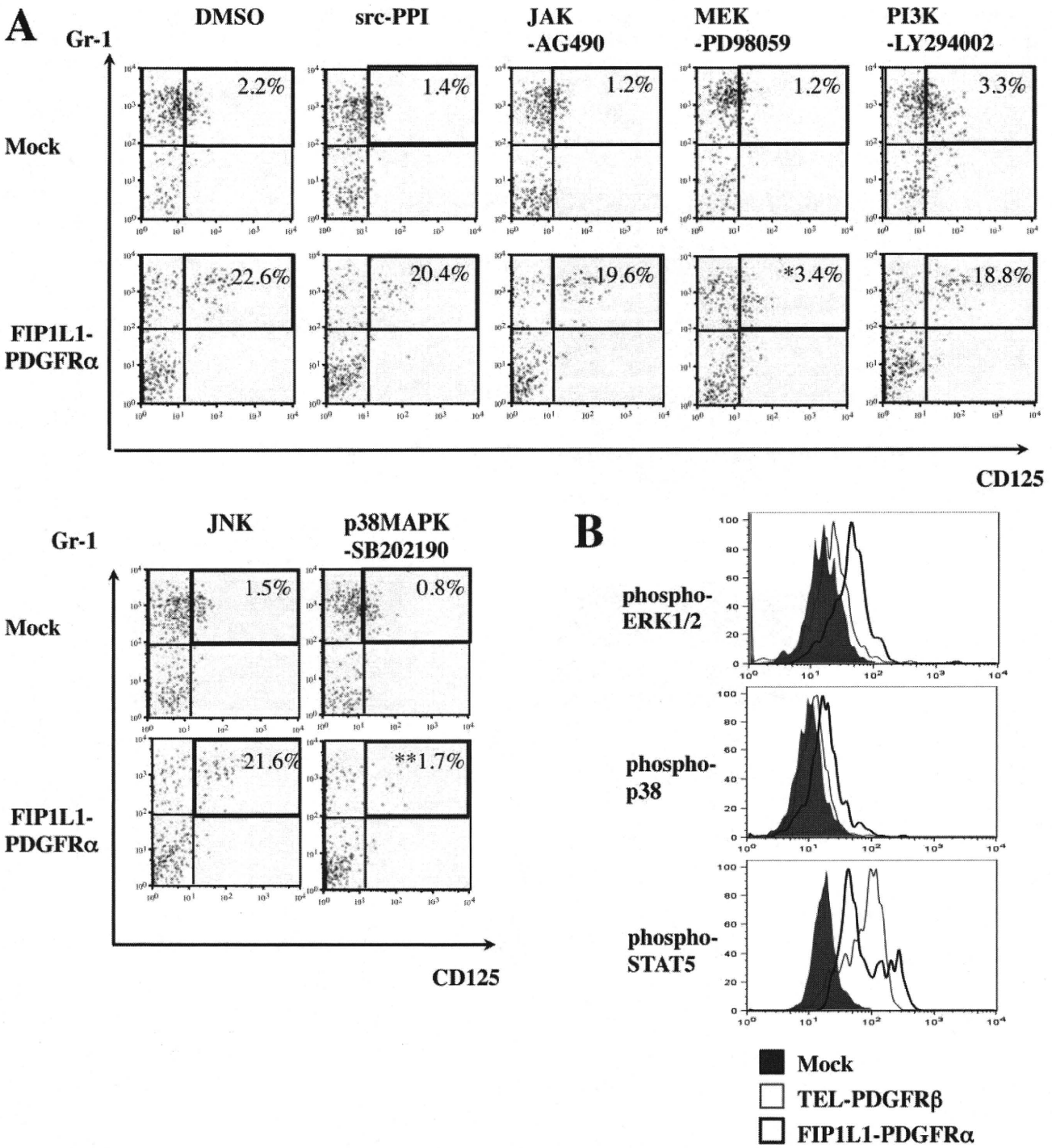

FIGURE 5. **Roles of signal cascades in FIP1L1-PDGFRα-induced eosinophil development.** *A*, murine KSLs were infected with the retrovirus indicated and cultured with SCF, TPO, IL-6, and FLT3L with or without kinase inhibitors as indicated and then subjected to FACS analysis. *, $p < 0.05$; **, $p < 0.01$ compared with the value of DMSO-treated cells ($n = 4$). *B*, FIP1L1-PDGFRα-, TEL-PDGFRβ-, or mock- transduced KSLs were cultured for 2 days, and the phosphorylation status of ERK1/2, p38MAPK, and STAT5 was analyzed using Phosflow technology.

not mock- or TEL-PDGFRβ-transduced CLPs aberrantly differentiate into Gr-1$^+$CD125$^+$ cells (percentage of Gr-1$^+$CD125$^+$ cells as follows: FIP1L1-PDGFRα, 57% *versus* mock (1%) ($p < 0.01$); TEL-PDGFRβ, 0% (Fig. 3*F*). We further cultured Gr-1$^+$CD125$^+$ cells that developed from FIP1L1-PDGFRα-transduced CLPs with a cytokine mixture containing IL-5 and confirmed that these cells became positive for eosinostain (data not shown). These results indicate that FIP1L1-PDGFRα inhibits B-lymphoid differentiation from CLPs and instructs them to differentiate into the eosinophil lineage.

Function of FIP1L1 and PDGFRα in the Fusion Protein—It was previously shown that the FIP1L1 moiety is dispensable

for kinase activation and for transforming properties of FIP1L1-PDGFRα (42). To determine the role of FIP1L1 in FIP1L1-PDGFRα-enhanced eosinophil development, we generated two artificial chimeric constructs, *FIP1L1-PDGFRβ* and *TEL-PDGFRα*, in which *FIP1L1* in *FIP1L1-PDGFRα* and *TEL* in *TEL-PDGFRβ* were completely replaced (Fig. 4*A*). In addition,

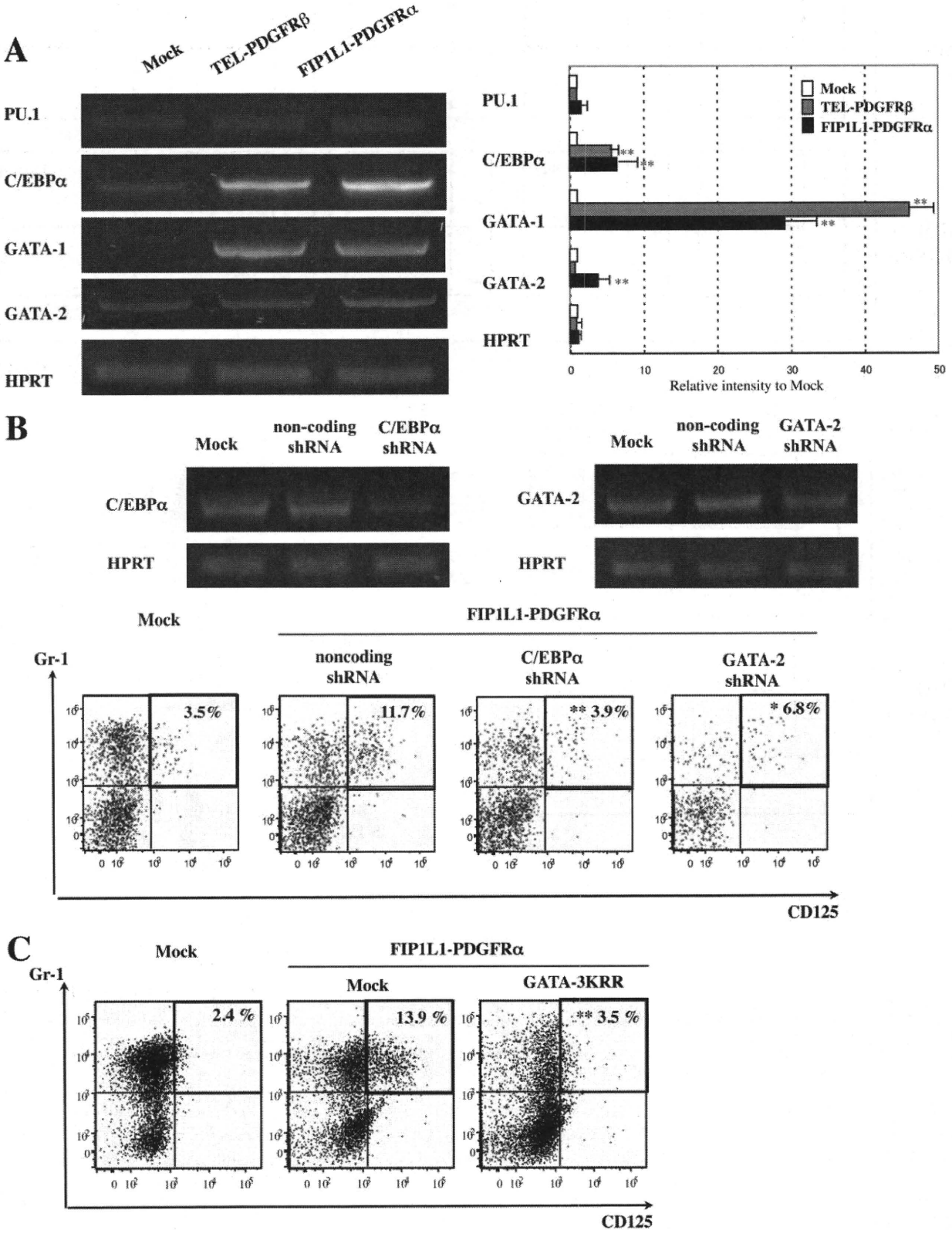

we generated retrovirus vectors for constitutively active PDGFRα (PDGFRαV561D and PDGFRαD842V), which are considered to be causative mutations of gastrointestinal stromal tumors (43) (Fig. 4*A*). When expressed in a murine IL-3-dependent cell line, Ba/F3, all of the four PDGFR mutants conferred IL-3-independent growth on these cells (data not shown). Also, Western blot analysis demonstrated that these PDGFR mutants phosphorylated various cellular proteins, including themselves (data not shown), indicating that these proteins act as constitutively active tyrosine kinases.

We transduced these retrovirus expression vectors into KSLs and cultured them with SCF, TPO, FLT3L, and IL-6 for 6 days. As shown in Fig. 4*B*, only TEL-PDGFRα and not FIP1L1-PDGFRβ, PDGFRαV561D, or PDGFRαD842V promoted eosinophil development from KSLs (percentage of Gr-1$^+$CD125$^+$ fraction as follows: TEL-PDGFRα, 74%; FIP1L1-PDGFRβ, 11%; PDGFRαV561D, 11%; PDGFRαD842V, 16%) (TEL-PDGFRα *versus* mock, $p < 0.01$) (Fig. 4*B*), indicating that FIP1L1 is dispensable for FIP1L1-PDGFRα-mediated eosinophil development and that PDGFRα-mediated signaling but not PDGFRβ-mediated signaling is required for inducing eosinophil development. However, because neither PDGFRαV561D nor PDGFRαD842V promoted eosinophil development, specific kinase activity transmitted from chimeric PDGFRα was supposed to be necessary to enhance eosinophil development.

Both a MEK1/2 Inhibitor and a p38^{MAPK} Inhibitor Blocked FIP1L1/PDGFRα-induced Eosinophil Development from KSLs—PDGFRα activates various downstream cascades, thereby exerting its biologic activity (44). To seek out the mechanism underlying instructive eosinophil differentiation induced by FIP1L1-PDGFRα, FIP1L1-PDGFRα- or mock-transduced KSLs were cultured with or without several kinase inhibitors as indicated (Fig. 5*A*).

As shown in Fig. 5*A* (*top*), neither a c-Jun N-terminal kinase inhibitor, a phosphatidylinositol 3-kinase inhibitor (LY294002), an Src inhibitor (PPI), nor a JAK2/STAT inhibitor (AG490) influenced FIP1L1-PDGFRα-enhanced eosinophil development, since about 20% of cells came to be CD125$^+$Gr1$^+$ after 5-day cultures as was seen after the culture without an inhibitor (Fig. 2*A*). In contrast, a MEK inhibitor (PD98059) and a p38^{MAPK} inhibitor (SB202190) reduced the CD125$^+$Gr1$^+$ fraction to 3.4% ($p < 0.05$) and 1.7% ($p < 0.01$), respectively (Fig. 5*A*, *bottom*). We also analyzed the phosphorylation states of ERK, STAT5, and p38^{MAPK} in FIP1L1-PDGFRα- or TEL-PDGFRβ-transduced KSLs by flow cytometry. As shown in Fig. 5*B*, ERK1/2 and p38MAPK but not STAT5 were phosphorylated more intensely in FIP1L1-PDGFRα-transduced KSLs than in mock- or TEL-PDGFRβ-transduced KSLs. These data suggest that FIP1L1-PDGFRα instructs HSCs/HPCs to differentiate into eosinophil progenitors through the activation of MEK1/2-ERK1/2 and p38 pathways.

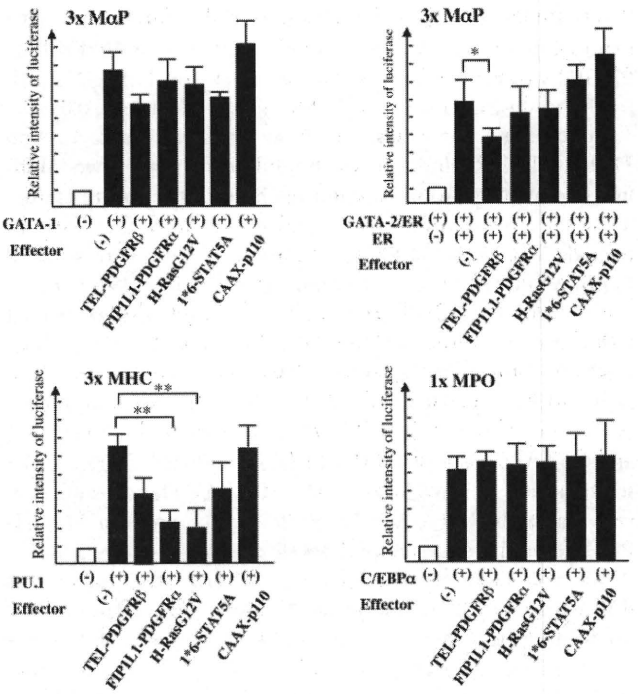

FIGURE 7. **Effects of FIP1L1-PDGFRα and its downstream molecules on the activities of eosinophil-related transcription factors.** The activities of GATA-1, GATA-2, PU.1, and C/EBPα were analyzed by luciferase assays. After transfection of several effector genes and the appropriate reporter genes, as indicated, NIH3T3 cells were cultured for 48 h and subjected to luciferase assays. 3×MαP-luciferase, 3×MHC-luciferase, and 1×MPO-luciferase contain biding sites for GATA, PU.1, and C/EBPα, respectively. *, $p < 0.05$; **, $p < 0.01$. Data represent means ± S.D. ($n = 3$).

Effects of FIP1L1-PDGFRα on the Expression and Activity of Lineage-specific Transcription Factors in KSLs—To further clarify the mechanism through which FIP1L1-PDGFRα enhanced eosinophil development, we analyzed the effects of FIP1L1-PDGFRα on the expression of *GATA-1*, *GATA-2*, *C/EBPα*, and *PU.1*, all of which have been reported to be key transcription factors for eosinophil development (45–47). To detect the changes in the expression of these factors that precede the phenotypic change, we isolated mRNA from sorted GFP-positive KSLs after 48-h retrovirus infection and performed semiquantitative RT-PCR analysis, since an apparent phenotypic change was not observed until 4 days (Fig. 2*A*, *top*). As shown in Fig. 6*A*, although the expression of *PU.1* was not so different among three transfectants, FIP1L1-PDGFRα augmented the expression of *C/EBPα* ($p < 0.01$) and *GATA-1* ($p <$

FIGURE 6. **Effects of FIP1L1-PDGFRα and its downstream molecules on the expressions of eosinophil-related transcription factors and effects of inhibition of these molecules.** *A*, the expressions of eosinophil-related transcription factors in KSLs were analyzed by RT-PCR analysis 48 h after retrovirus transfection. PCR products were electrophoresed and visualized by ethidium bromide staining (*left*), and their intensities were quantified using a Fluor Imager595 and ImageQuant software. Relative intensities to the products from mock-transduced cells are indicated (*right*). *, $p < 0.05$; **, $p < 0.01$ as compared with the value in mock-transduced cells. Data represent means ± S.D. ($n = 3$). *B*, murine KSLs were infected with lentivirus-expressing noncoding or encoding shRNA against C/EBPα or GATA-2 to evaluate the suppression efficacy of each shRNA. After a 48-h culture, cells were subjected to RT-PCR analyses (*top*). Next, FIP1L1-PDGFRα-transduced murine KSLs were further infected with these shRNAs and cultured with SCF, TPO, IL-6, and FLT3L, which were subjected to FACS analyses upon the expression of CD125 and Gr-1 (*bottom*). *, $p < 0.05$; **, $p < 0.01$ as compared with the value in the cells coexpressing FIP1L1-PDGFRα and noncoding shRNA ($n = 3$). *C*, FIP1L1-PDGFRα-transduced murine KSLs were further infected with retrovirus encoding mock or a dominant negative form of GATAs (GATA-3KRR). **, $p < 0.01$ as compared with the value in FIP1L1-PDGFRα- and mock-cotransduced cells ($n = 3$).

0.01) compared with mock-transduced KSLs. Furthermore, the expression of *GATA-2* was significantly higher in FIP1L1-PDGFRα-transduced KSLs than in mock- or TEL-PDGFRβ-transduced KSLs (FIP1L1-PDGFRα *versus* mock, $p < 0.01$).

To evaluate the roles for these transcription factors in FIP1L1-PDGFRα-induced eosinophil development, we inhibited the expression or function of these transcription factors using shRNAs or a dominant negative mutant. At first, we confirmed that these shRNAs suppressed the expression of *C/EBPα* and *GATA-2* considerably (Fig. 6*B*, *top*). When coexpressed with FIP1L1-PDGFRα in this condition, shRNA against C/EBPα reduced the FIP1L1-PDGFRα-induced $CD125^+Gr1^+$ fraction from 11.7 to 3.9% ($p < 0.01$) (Fig. 6*B*, *bottom*). Similarly, shRNA against GATA-2 suppressed this fraction to 6.8% ($p < 0.05$). Also, *GATA-3KRR*, which can inhibit both GATA-1 and GATA-2, reduced FIP1L1-PDGFRα-induced $CD125^+Gr1^+$ fraction from 13.9 to 3.5% ($p < 0.01$) (Fig. 6*C*). These results indicate that both GATA-2 and C/EBPα are required for FIP1L1-PDGFRα-induced eosinophil development.

We also examined the effects of FIP1L1-PDGFRα and its downstream signaling molecules (*i.e.* Ras, STAT5, and PI3-K) on transcription activities of these factors with luciferase assays using reporter genes and effector genes in combinations, as indicated in Fig. 7. In NIH3T3 cells, transiently transduced reporter genes for GATAs (3×*MαP*-luciferase), PU.1 (3×*MHC*-luciferase), and C/EBPα (1×*MPO*-luciferase) were activated by cotransfected GATA-1, PU.1, and C/EBPα by 7-fold, 7-fold, and 5-fold, respectively (Fig. 7). Also, the estradiol treatment activated 3×*MαP*-luciferase in GATA-2/ER-transfected cells. When FIP1L1-PDGFRα or a constitutively active form of H-Ras (H-RasG12V), STAT5 (1*6-STAT5A), or phosphatidylinositol 3-kinase (CAAX-p110) was further cotransfected, 1*6-STAT5A and CAAX-p110 scarcely affected transcription activities of GATA-1, GATA-2, PU.1, and C/EBPα. In contrast, both FIP1L1-PDGFRα and H-RasG12V reduced PU.1 activities to 30–40% ($p < 0.01$). Similar results were also obtained from 293T cells (data not shown). These results indicate that FIP1L1-PDGFRα regulates the expression and activities of various transcription factors, thereby promoting eosinophil development, and suggest that Ras may be a pivotal downstream mediator of FIP1L1-PDGFRα in this process.

DISCUSSION

In this study, we found that TEL-PDGFRα, but not FIP1L1-PDGFRβ, PDGFRαD562V, or PDGFRαD842V, promoted eosinophil development from KSLs as efficiently as FIP1L1-PDGFRα. This result indicates that constitutive TK activity transmitted from chimeric structure of PDGFRα is necessary to augment eosinophil development. In agreement with our finding, novel mutations identified in CEL were restricted to the chimeric form of PDGFRα (*i.e.* KIF5B-PDGFRα formed by t(4;10)(q12;p11), STRN-PDGFRα by t(2;4)(p24;q12), and ETV6-PDGFRα by t(4;12)(q2?3;p1?2)). As for the roles for downstream signaling molecules, the current results indicate that Ras/MEK and $p38^{MAPK}$ play essential roles in FIP1L1-PDGFRα-induced eosinophil development. However, this finding seems to be inconsistent with the fact that Ras/MEK is activated by various LTKs and normal hematopoietic growth factors. As for this reason, because FIP1L1-PDGFRα more intensely activated MEK/ERK and $p38^{MAPK}$ than TEL-PDGFRβ, we speculated that leukemogenic signals transmitted from chimeric PDGFRα would be quantitatively and qualitatively different from those from wild type TKs or other LTKs, thereby specifically promoting eosinophil development. In addition to the regulation of neoplastic cell proliferation, ERK has also been implicated in the control of signaling cascades associated with eosinophilia in asthma. Duan *et al.* (48) reported that an MEK inhibitor dramatically inhibited OVA-induced lung tissue eosinophilia and airway hyperresponsiveness. Also, $p38^{MAPK}$ is important for the induction of eosinophilia and function of terminal differentiated eosinophils in allergic airway inflammation (49, 50). In addition, our data suggest that $p38^{MAPK}$ would regulate eosinophil development at the early stage of hematopoiesis. Further studies to elucidate the crucial signal transduction mechanisms that control eosinophil development will provide a better rationale for the design of drug therapy not only for FIP1L1-PDGFRα-associated HES/CEL but also for allergic inflammation.

Our *in vitro* studies showed that FIP1L1-PDGFRα confers cytokine independence on KSLs and enhances their self-renewal activity, whereas it did not immortalize CMPs. In addition, although FIP1L1-PDGFRα-transduced KSLs caused MPD in recipient mice, FIP1L1-PDGFRα-transduced CMPs did not. These results indicate that FIP1L1-PDGFRα cannot confer self-renewal activity on CMPs and that the genetic alternation of FIP1L1-PDGFRα that causes CEL/HES occurs at an HSC level but not at a CMP level. In addition, we confirmed that mature eosinophils were generated from FIP1L1-PDGFRα-transduced KSLs in the presence of IL-5, indicating that FIP1L1-PDGFRα does not impair terminal differentiation of eosinophils. Also, when expressed in MEPs or CLPs, FIP1L1-PDGFRα brought about lineage conversion to eosinophil lineage. Together, these results suggest that, although LSCs harboring FIP1L1-PDGFRα derived from HSCs would continuously produce an excess number of mature eosinophils, a part of the eosinophils might be derived from FIP1L1-PDGFRα-harboring MEPs or CLPs.

In a previous report, FIP1L1-PDGFRα-transduced HSCs/HPCs caused myeloproliferative disorder in the recipient mice like BCR-ABL- or TEL-PDGFRβ-transduced KSLs (16, 51, 52), which was rather different from simple eosinophilia observed in human HES/CEL. Also in our transplantation experiment, none of the five mice transplanted with FIP1L1-PDGFRα-expressing KSLs developed eosinophilic disorders. However, we also observed that, whereas FIP1L1-PDGFRα-introduced KSLs differentiated up to $IL\text{-}5R\alpha^+$ eosinophil precursors under the cultures without IL-5, supplement of IL-5 let these $IL\text{-}5R\alpha^+$ cells undergo eosinophilic terminal differentiation. In accord with this hypothesis, Yamada *et al.* (52) reported that transplantation of FIP1L1-PDGFRα-transduced HSCs/HPCs obtained from IL-5 transgenic mice resulted in marked eosinophilia resembling HES/CEL in the recipient mice. Since p210BCR-ABL-transduced HSCs/HPCs did not cause eosinophilia even in the presence of IL-5 overexpression in the recipient mice, the induction of eosinophilia was attributable to FIP1L1-PDGFRα, Together with our results, these lines of evidence suggest that, although FIP1L1-PDGFRα is a major etiologic factor causing

eosinophilia, it is not sufficient to induce HES/CEL but requires additional events, such as IL-5 overexpression. In fact, some patients with FIP1L1-PDGFRα-associated HES were complicated with T-cell lymphoma (53–55). The frequency of FIP1L1-PDGFRα-induced HES/CEL was not as high (about 10%) as initially reported. However, similar LTK is supposed to be involved in the pathogenesis of HES/CEL, because imatinib is effective in some patients who do not have a *FIP1L1-PDGFRα* mutation (56). Also, a significant proportion of patients with HES/CEL have abnormal T-lymphocyte populations, such as $CD3^+CD4^-CD8^-$ and $CD3^-CD8^+$ T cells, which secret high levels of IL-5 (57). Currently, HES is categorized into two groups, "myeloproliferative variant" and "T-cell-mediated HES," and these groups are thought to be independent of each other (58, 59). However, because T-cell differentiation might be perturbed by FIP1L1-PDGFRα, it may be meaningful for the better understanding of the pathogenesis of HES/CEL to clarify the relationship between these two groups.

Iwasaki *et al.* (60) isolated eosinophil progenitors from murine BM, and they concluded that eosinophil developmental pathway would diverge from neutrophils and monocytes at the GMP stage. The lineage commitment of HSCs/HPCs and subsequent lineage-specific differentiation are crucially regulated by lineage-specific transcription factors, such as GATA-1, GATA-3, PU.1, C/EBPα, and C/EBPε. Among them, GATA-1 and PU.1 are known to antagonize each other and induce differentiation to erythroid/megakalyocyte or myeloid lineage, respectively (61–63). The CEBP family (CEBPα and CEBPε) is essential for the differentiation to myeloid lineage (64–66). FOG (Friend of GATA) and C/EBPβ regulate the eosinophil lineage induction antagonistically (67). Furthermore, enforced expression of C/EBPα converts MEPs to eosinophils (68), and expression of PU.1 converts them to GMPs (61, 67). Also, forced expression of GATA-1 in myeloid cells induces the formation of either MEPs or eosinophils, depending on the concentration of the factor (69). In addition, it was recently reported that C/EBPα expression followed by GATA-2 expression in GMPs is critical for eosinophil lineage specification (46). However, it is plausible that the mechanism of lineage commitment in leukemic cells is somewhat different from that in normal hematopoietic cells. In this study, we found that FIP1L1-PDGFRα enhanced the expression of GATA-1, GATA-2, and C/EBPα and suppressed PU.1 expression. Also, FIP1L1-PDGFRα suppressed transcription activities of PU.1. These results suggest that LTKs can influence the lineage commitment of HSCs/HPCs and subsequent differentiation by modifying the expression and activity of lineage-specific transcription factors.

In conclusion, we here found that FIP1L1-PDGFRα can enhance eosinophil development from HSCs/HPCs through the MEK/ERK and $p38^{MAPK}$ cascades by controlling the expression and activity of lineage-specific transcription factors. Furthermore, as far as we explored, this is the first report providing evidence that LTK has an ability to convert the lineage of committed progenitor cells. Further studies based on these findings would undoubtedly provide more useful information to understand the pathophysiology of various hematologic malignancies caused by LTKs.

Acknowledgments—We thank Dr. Gary Gilliland for provision of plasmids encoding FIP1L1-PDGFRα and TEL-PDGFRβ, Dr. Seiichi Hirota for provision of the plasmids encoding mutated PDGFRαs, and Dr. Hiroyuki Miyoshi for provision of 293gp cells.

REFERENCES

1. Semerad, C. L., Poursine-Laurent, J., Liu, F., and Link, D. C. (1999) *Immunity* **11,** 153–161
2. Arcasoy, M. O., Maun, N. A., Perez, L., Forget, B. G., and Berliner, N. (2001) *Eur. J. Haematol.* **67,** 77–87
3. Hsu, C. L., Kikuchi, K., and Kondo, M. (2007) *Blood* **110,** 1420–1428
4. Buitenhuis, M., Verhagen, L. P., van Deutekom, H. W., Castor, A., Verploegen, S., Koenderman, L., Jacobsen, S. E., and Coffer, P. J. (2008) *Blood* **111,** 112–121
5. Radomska, H. S., Basseres, D. S., Zheng, R., Zhang, P., Dayaram, T., Yamamoto, Y., Sternberg, D. W., Lokker, N., Giese, N. A., Bohlander, S. K., Schnittger, S., Delmotte, M. H., Davis, R. J., Small, D., Hiddemann, W., Gilliland, D. G., and Tenen, D. G. (2006) *J. Exp. Med.* **203,** 371–381
6. Yamamoto, Y., Kiyoi, H., Nakano, Y., Suzuki, R., Kodera, Y., Miyawaki, S., Asou, N., Kuriyama, K., Yagasaki, F., Shimazaki, C., Akiyama, H., Saito, K., Nishimura, M., Motoji, T., Shinagawa, K., Takeshita, A., Saito, H., Ueda, R., Ohno, R., and Naoe, T. (2001) *Blood* **97,** 2434–2439
7. Levis, M., Tse, K. F., Smith, B. D., Garrett, E., and Small, D. (2001) *Blood* **98,** 885–887
8. Griffith, J., Black, J., Faerman, C., Swenson, L., Wynn, M., Lu, F., Lippke, J., and Saxena, K. (2004) *Mol. Cell.* **13,** 169–178
9. Bene, M. C., Bernier, M., Casasnovas, R. O., Castoldi, G., Knapp, W., Lanza, F., Ludwig, W. D., Matutes, E., Orfao, A., Sperling, C., and van't Veer, M. B. (1998) *Blood* **92,** 596–599
10. Nagata, H., Worobec, A. S., Oh, C. K., Chowdhury, B. A., Tannenbaum, S., Suzuki, Y., and Metcalfe, D. D. (1995) *Proc. Natl. Acad. Sci. U. S. A.* **92,** 10560–10564
11. Longley, B. J., Tyrrell, L., Lu, S. Z., Ma, Y. S., Langley, K., Ding, T. G., Duffy, T., Jacobs, P., Tang, L. H., and Modlin, I. (1996) *Nat. Genet.* **12,** 312–314
12. Ikeda, H., Kanakura, Y., Tamaki, T., Kuriu, A., Kitayama, H., Ishikawa, J., Kanayama, Y., Yonezawa, T., Tarui, S., and Griffin, J. D. (1991) *Blood* **78,** 2962–2968
13. Longley, B. J., Jr., Metcalfe, D. D., Tharp, M., Wang, X., Tyrrell, L., Lu, S. Z., Heitjan, D., and Ma, Y. (1999) *Proc. Natl. Acad. Sci. U. S. A.* **96,** 1609–1614
14. Fritsche-Polanz, R., Jordan, J. H., Feix, A., Sperr, W. R., Sunder-Plassmann, G., Valent, P., and Fodinger, M. (2001) *Br. J. Haematol.* **113,** 357–364
15. Furitsu, T., Tsujimura, T., Tono, T., Ikeda, H., Kitayama, H., Koshimizu, U., Sugahara, H., Butterfield, J. H., Ashman, L. K., Kanayama, Y., Matsuzawa, Y., Kitamura, Y., and Kanakura, Y. (1993) *J. Clin. Invest.* **92,** 1736–1744
16. Cools, J., Stover, E. H., Boulton, C. L., Gotlib, J., Legare, R. D., Amaral, S. M., Curley, D. P., Duclos, N., Rowan, R., Kutok, J. L., Lee, B. H., Williams, I. R., Coutre, S. E., Stone, R. M., DeAngelo, D. J., Marynen, P., Manley, P. W., Meyer, T., Fabbro, D., Neuberg, D., Weisberg, E., Griffin, J. D., and Gilliland, D. G. (2003) *Cancer Cell* **3,** 459–469
17. Klion, A. D., Noel, P., Akin, C., Law, M. A., Gilliland, D. G., Cools, J., Metcalfe, D. D., and Nutman, T. B. (2003) *Blood* **101,** 4660–4666
18. Stover, E. H., Chen, J., Lee, B. H., Cools, J., McDowell, E., Adelsperger, J., Cullen, D., Coburn, A., Moore, S. A., Okabe, R., Fabbro, D., Manley, P. W., Griffin, J. D., and Gilliland, D. G. (2005) *Blood* **106,** 3206–3213
19. Cools, J., DeAngelo, D. J., Gotlib, J., Stover, E. H., Legare, R. D., Cortes, J., Kutok, J., Clark, J., Galinsky, I., Griffin, J. D., Cross, N. C., Tefferi, A., Malone, J., Alam, R., Schrier, S. L., Schmid, J., Rose, M., Vandenberghe, P., Verhoef, G., Boogaerts, M., Wlodarska, I., Kantarjian, H., Marynen, P., Coutre, S. E., Stone, R., and Gilliland, D. G. (2003) *N. Engl. J. Med.* **348,** 1201–1214
20. Griffin, J. H., Leung, J., Bruner, R. J., Caligiuri, M. A., and Briesewitz, R. (2003) *Proc. Natl. Acad. Sci. U. S. A.* **100,** 7830–7835
21. La Starza, R., Specchia, G., Cuneo, A., Beacci, D., Nozzoli, C., Luciano, L., Aventin, A., Sambani, C., Testoni, N., Foppoli, M., Invernizzi, R., Marynen, P., Martelli, M. F., and Mecucci, C. (2005) *Haematologica* **90,**

596–601
22. Buitenhuis, M., Verhagen, L. P., Cools, J., and Coffer, P. J. (2007) *Cancer Res.* **67,** 3759–3766
23. Bonnet, D., and Dick, J. E. (1997) *Nat. Med.* **3,** 730–737
24. Hope, K. J., Jin, L., and Dick, J. E. (2004) *Nat. Immunol.* **5,** 738–743
25. Sutherland, H. J., Blair, A., and Zapf, R. W. (1996) *Blood* **87,** 4754–4761
26. Blair, A., Hogge, D. E., and Sutherland, H. J. (1998) *Blood* **92,** 4325–4335
27. Cozzio, A., Passegue, E., Ayton, P. M., Karsunky, H., Cleary, M. L., and Weissman, I. L. (2003) *Genes Dev.* **17,** 3029–3035
28. Huntly, B. J., Shigematsu, H., Deguchi, K., Lee, B. H., Mizuno, S., Duclos, N., Rowan, R., Amaral, S., Curley, D., Williams, I. R., Akashi, K., and Gilliland, D. G. (2004) *Cancer Cell* **6,** 587–596
29. Akashi, K., Traver, D., Miyamoto, T., and Weissman, I. L. (2000) *Nature* **404,** 193–197
30. Segawa, K., Matsuda, M., Fukuhara, A., Morita, K., Okuno, Y., Komuro, R., and Shimomura, I. (2009) *J. Endocrinology* **200,** 107–116
31. Okitsu, Y., Takahashi, S., Minegishi, N., Kameoka, J., Kaku, M., Yamamoto, M., Sasaki, T., and Harigae, H. (2007) *Biochem. Biophys. Res. Commun.* **364,** 383–387
32. Smith, V. M., Lee, P. P., Szychowski, S., and Winoto, A. (1995) *The J. Biol. Chem.* **270,** 1515–1520
33. Ezoe, S., Matsumura, I., Nakata, S., Gale, K., Ishihara, K., Minegishi, N., Machii, T., Kitamura, T., Yamamoto, M., Enver, T., and Kanakura, Y. (2002) *Blood* **100,** 3512–3520
34. Ono, R., Ihara, M., Nakajima, H., Ozaki, K., Kataoka-Fujiwara, Y., Taki, T., Nagata, K., Inagaki, M., Yoshida, N., Kitamura, T., Hayashi, Y., Kinoshita, M., and Nosaka, T. (2005) *Mol. Cell. Biol.* **25,** 10965–10978
35. Ezoe, S., Matsumura, I., Gale, K., Satoh, Y., Ishikawa, J., Mizuki, M., Takahashi, S., Minegishi, N., Nakajima, K., Yamamoto, M., Enver, T., and Kanakura, Y. (2005) *J. Biol. Chem.* **280,** 13163–13170
36. Matsumura, I., Kawasaki, A., Tanaka, H., Sonoyama, J., Ezoe, S., Minegishi, N., Nakajima, K., Yamamoto, M., and Kanakura, Y. (2000) *Blood* **96,** 2440–2450
37. Matsumura, I., Kitamura, T., Wakao, H., Tanaka, H., Hashimoto, K., Albanese, C., Downward, J., Pestell, R. G., and Kanakura, Y. (1999) *EMBO J.* **18,** 1367–1377
38. Doornbos, R. P., Theelen, M., van der Hoeven, P. C., van Blitterswijk, W. J., Verkleij, A. J., and van Bergen en Henegouwen, P. M. (1999) *J. Biol. Chem.* **274,** 8589–8596
39. Tanaka, H., Matsumura, I., Itoh, K., Hatsuyama, A., Shikamura, M., Satoh, Y., Heike, T., Nakahata, T., and Kanakura, Y. (2006) *Stem Cells* **24,** 2592–2602
40. Abkowitz, J. L., Golinelli, D., Harrison, D. E., and Guttorp, P. (2000) *Blood* **96,** 3399–3405
41. Huang, S., Law, P., Francis, K., Palsson, B. O., and Ho, A. D. (1999) *Blood* **94,** 2595–2604
42. Stover, E. H., Chen, J., Folens, C., Lee, B. H., Mentens, N., Marynen, P., Williams, I. R., Gilliland, D. G., and Cools, J. (2006) *Proc. Natl. Acad. Sci. U. S. A.* **103,** 8078–8083
43. Heinrich, M. C., Corless, C. L., Duensing, A., McGreevey, L., Chen, C. J., Joseph, N., Singer, S., Griffith, D. J., Haley, A., Town, A., Demetri, G. D., Fletcher, C. D., and Fletcher, J. A. (2003) *Science* **299,** 708–710
44. Heldin, C. H., and Westermark, B. (1999) *Physiol. Rev.* **79,** 1283–1316
45. McNagny, K., and Graf, T. (2002) *J. Exp. Med.* **195,** F43–F47
46. Iwasaki, H., Mizuno, S., Arinobu, Y., Ozawa, H., Mori, Y., Shigematsu, H., Takatsu, K., Tenen, D. G., and Akashi, K. (2006) *Genes Dev.* **20,** 3010–3021
47. Du, J., Stankiewicz, M. J., Liu, Y., Xi, Q., Schmitz, J. E., Lekstrom-Himes, J. A., and Ackerman, S. J. (2002) *J. Biol. Chem.* **277,** 43481–43494
48. Duan, W., Chan, J. H., Wong, C. H., Leung, B. P., and Wong, W. S. (2004) *J. Immunol.* **172,** 7053–7059
49. Kampen, G. T., Stafford, S., Adachi, T., Jinquan, T., Quan, S., Grant, J. A., Skov, P. S., Poulsen, L. K., and Alam, R. (2000) *Blood* **95,** 1911–1917
50. Wong, C. K., Zhang, J. P., Ip, W. K., and Lam, C. W. (2002) *Clin. Exp. Immunol.* **128,** 483–489
51. Daley, G. Q., Van Etten, R. A., and Baltimore, D. (1990) *Science* **247,** 824–830
52. Yamada, Y., Rothenberg, M. E., Lee, A. W., Akei, H. S., Brandt, E. B., Williams, D. A., and Cancelas, J. A. (2006) *Blood* **107,** 4071–4079
53. McPherson, T., Cowen, E. W., McBurney, E., and Klion, A. D. (2006) *Br. J. Dermatol.* **155,** 824–826
54. Robyn, J., Lemery, S., McCoy, J. P., Kubofcik, J., Kim, Y. J., Pack, S., Nutman, T. B., Dunbar, C., and Klion, A. D. (2006) *Br. J. Haematol.* **132,** 286–292
55. Capovilla, M., Cayuela, J. M., Bilhou-Nabera, C., Gardin, C., Letestu, R., Baran-Marzak, F., Fenaux, P., and Martin, A. (2008) *Eur. J. Haematol.* **80,** 81–86
56. Jovanovic, J. V., Score, J., Waghorn, K., Cilloni, D., Gottardi, E., Metzgeroth, G., Erben, P., Popp, H., Walz, C., Hochhaus, A., Roche-Lestienne, C., Preudhomme, C., Solomon, E., Apperley, J., Rondoni, M., Ottaviani, E., Martinelli, G., Brito-Babapulle, F., Saglio, G., Hehlmann, R., Cross, N. C., Reiter, A., and Grimwade, D. (2007) *Blood* **109,** 4635–4640
57. Simon, H. U., Plotz, S. G., Dummer, R., and Blaser, K. (1999) *N. Engl. J. Med.* **341,** 1112–1120
58. Roufosse, F., Cogan, E., and Goldman, M. (2003) *Annu. Rev. Med.* **54,** 169–184
59. Roufosse, F. E., Goldman, M., and Cogan, E. (2003) *N. Engl. J. Med.* **348,** 2687; Author Reply 2687
60. Iwasaki, H., Mizuno, S., Mayfield, R., Shigematsu, H., Arinobu, Y., Seed, B., Gurish, M. F., Takatsu, K., and Akashi, K. (2005) *J. Exp. Med.* **201,** 1891–1897
61. Rekhtman, N., Radparvar, F., Evans, T., and Skoultchi, A. I. (1999) *Genes Dev.* **13,** 1398–1411
62. Zhang, P., Behre, G., Pan, J., Iwama, A., Wara-Aswapati, N., Radomska, H. S., Auron, P. E., Tenen, D. G., and Sun, Z. (1999) *Proc. Natl. Acad. Sci. U. S. A.* **96,** 8705–8710
63. Nerlov, C., Querfurth, E., Kulessa, H., and Graf, T. (2000) *Blood* **95,** 2543–2551
64. Smith, L. T., Hohaus, S., Gonzalez, D. A., Dziennis, S. E., and Tenen, D. G. (1996) *Blood* **88,** 1234–1247
65. Hohaus, S., Petrovick, M. S., Voso, M. T., Sun, Z., Zhang, D. E., and Tenen, D. G. (1995) *Mol. Cell. Biol.* **15,** 5830–5845
66. Wang, N. D., Finegold, M. J., Bradley, A., Ou, C. N., Abdelsayed, S. V., Wilde, M. D., Taylor, L. R., Wilson, D. R., and Darlington, G. J. (1995) *Science* **269,** 1108–1112
67. Querfurth, E., Schuster, M., Kulessa, H., Crispino, J. D., Doderlein, G., Orkin, S. H., Graf, T., and Nerlov, C. (2000) *Genes Dev.* **14,** 2515–2525
68. McNagny, K. M., and Graf, T. (2003) *Blood* **101,** 1103–1110
69. Kulessa, H., Frampton, J., and Graf, T. (1995) *Genes Dev.* **9,** 1250–1262

Notch2 signaling is required for proper mast cell distribution and mucosal immunity in the intestine

Mamiko Sakata-Yanagimoto,[1,2] Toru Sakai,[3] Yasuyuki Miyake,[1] Toshiki I. Saito,[2,4] Haruhiko Maruyama,[5] Yasuyuki Morishita,[6] Etsuko Nakagami-Yamaguchi,[2] Keiki Kumano,[2,7] Hideo Yagita,[8] Masashi Fukayama,[9] Seishi Ogawa,[9,10] Mineo Kurokawa,[7] Koji Yasutomo,[3] and Shigeru Chiba[1,2]

[1]Department of Clinical and Experimental Hematology, University of Tsukuba, Tsukuba, Japan; [2]Department of Cell Therapy and Transplantation Medicine, University of Tokyo Hospital, Tokyo, Japan; [3]Department of Immunology and Parasitology, Institute of Health Biosciences, The University of Tokushima Graduate School, Tokushima, Japan; [4]Laboratory of Cell Therapy, Department of Regenerative Medicine, Clinical Research Center, National Hospital Organization Nagoya Medical Center, Nagoya, Japan; [5]Parasitic Diseases Unit, Department of Infectious Diseases, Faculty of Medicine, University of Miyazaki, Miyazaki, Japan; [6]Department of Pathology, University of Tokyo, Tokyo, Japan; [7]Department of Hematology and Oncology, University of Tokyo, Tokyo, Japan; [8]Department of Immunology, Juntendo University School of Medicine, Tokyo, Japan; [9]Cancer Genomics Project, Graduate School of Medicine, University of Tokyo, Tokyo, Japan; and [10]Core Research for Evolutional Science and Technology, Japan Science and Technology Agency, Tokyo, Japan

Notch receptor-mediated signaling is involved in the developmental process and functional modulation of lymphocytes, as well as in mast cell differentiation. Here, we investigated whether Notch signaling is required for antipathogen host defense regulated by mast cells. Mast cells were rarely found in the small intestine of wild-type C57BL/6 mice but accumulated abnormally in the lamina propria of the small-intestinal mucosa of the *Notch2*-conditional knockout mice in naive status. When transplanted into mast cell–deficient W^{sh}/W^{sh} mice, *Notch2*-null bone marrow-derived mast cells were rarely found within the epithelial layer but abnormally localized to the lamina propria, whereas control bone marrow-derived mast cells were mainly found within the epithelial layer. After the infection of *Notch2* knockout and control mice with L3 larvae of *Strongyloides venezuelensis*, the abundant number of mast cells was rapidly mobilized to the epithelial layer in the control mice. In contrast, mast cells were massively accumulated in the lamina propria of the small intestinal mucosa in *Notch2*-conditional knockout mice, accompanied by impaired eradication of *Strongyloides venezuelensis*. These findings indicate that cell-autonomous Notch2 signaling in mast cells is required for proper localization of intestinal mast cells and further imply a critical role of Notch signaling in the host-pathogen interface in the small intestine. (*Blood*. 2011;117(1):128-134)

Introduction

Mast cells are important in a wide variety of physiologic and pathologic processes, including protective immune responses to parasites and allergic disorders.[1,2] In intestinal parasite infection, mast cells play a central role in the immune response.[3] During the induction phase of parasite-induced inflammation, mast cells move from the submucosa to the tip of the villi, accompanying the serial changes in the protease expression pattern. Initially, they are positive for mouse mast cell protease-5 (mMCP-5) but negative for mMCP-1 and mMCP-2; eventually, they become positive for mMCP-1 and mMCP-2 but negative for mMCP-5, demonstrating convergence from connective tissue–type mast cells (CTMCs) to mature mucosal-type mast cells (MTMCs).[4] The parasite-infected mice consequently experience jejunal mast cell hyperplasia,[5] and the serum concentration of mMCP-1, an activation marker of small intestinal mast cells, is increased by > 1000-fold compared with that in the naive status.[5]

In the mammalian immune system, we and other groups have demonstrated that Notch signaling is involved in the commitment and differentiation of T cells, the development of splenic marginal zone B cells, and the differentiation and functional modulation of mature T cells, including T-helper type I (Th1)/Th2 polarization[6,7] and differentiation of CD8-positive cytotoxic T cells.[8] Regarding the Notch signaling in mast cells, bone marrow-derived mast cells (BMMCs) highly express Jagged1[9] and Notch2[10] among the Notch ligands and the receptors, respectively. We have previously shown that signaling through the Notch2 receptor induces mast cell development from myeloid progenitors by transcriptional up-regulation of hairy and enhancer of split homolog-1 (Hes-1) and transacting T cell–specific transcription factor GATA-3 (GATA3).[11] Induction of antigen-presenting potential of mast cells by Notch signaling is also demonstrated.[12] A question yet to be solved is how Notch signaling affects mast cell properties in vivo.

In this report, we examined the effect of Notch2 signaling in in vivo mast cells using *Notch2*-conditional knockout mice.[13] We show that Notch2 signaling is specifically required for intraepithelial localization of intestinal mast cells and antiparasite immunity. In contrast, Notch2 is dispensable for either distribution or development of CTMCs.

Submitted July 9, 2010; accepted September 28, 2010. Prepublished online as *Blood* First Edition paper, October 22, 2010; DOI 10.1182/blood-2010-07-289611.

The online version of this article contains a data supplement.

The publication costs of this article were defrayed in part by page charge payment. Therefore, and solely to indicate this fact, this article is hereby marked "advertisement" in accordance with 18 USC section 1734.

Methods

Mice

The generation of *Notch2*$^{flox/flox}$ mice was described previously.[13] Mx-*Cre* transgenic mice[14] were crossed with *Notch2*$^{flox/flox}$ mice (*N2*-MxcKO mice) and the progeny were injected with polyinosinic-polycytidylic acid (pIpC; Sigma-Aldrich) 7 times every other day from 3 days after birth (25 μg/g body weight) or 3 times between 4 and 6 weeks of age (20 μg/g body weight). *N2*-MxcKO mice were further crossed with C57BL/6-Ly5.1 mice (a kind gift from Dr H. Nakauchi, University of Tokyo) to generate Ly5.1-*N2*-MxcKO mice. *Notch2* deletion in bone marrow was examined by polymerase chain reaction and 3% agarose gel electrophoresis[13] (supplemental Figure 1, available on the *Blood* Web site; see the Supplemental Materials link at the top of the online article). *W*^{sh}/*W*^{sh} mice were purchased from The Jackson Laboratory. All experiments were done with approval from the University of Tsukuba Institutional Review Board.

Staining

Sections, fixed with Carnoid fluid, were stained with 0.5% toluidine blue (Sigma-Aldrich), pH 0.3, followed by eosin. Small intestine was embedded in optimal cutting temperature (OCT) compound (TissueTek) and cut with cryostat (Leica CM1850). The section was fixed with 4% paraformaldehyde, washed with phosphate-buffered saline (PBS), blocked in 10% horse serum and 0.1% Triton-PBS, and then stained with either 1:100 goat anti-Jagged1 antibody (C-20; Santa Cruz Biotechnology), goat anti-Delta1 antibody (Genzyme Tech), or control goat immunoglobulin G (IgG; Santa Cruz Biotechnology) overnight at 4°C. The sections were washed with PBS and stained with anti–goat Alexa 594 (Invitrogen). Sections were analyzed by fluorescence microscope (Zeiss; Axioplan2), original magnification ×200.

BMMCs

Bone marrow cells from each mouse strain were cultured in RPMI 1640 medium (Sigma-Aldrich) supplemented with 10% fetal bovine serum (FBS), 50 ng/mL stem cell factor (SCF; PeproTech), and 10 ng/mL interleukin-3 (IL-3; PeproTech) for 4 weeks. Generation of BMMCs was confirmed by staining with lineage markers, c-Kit and IgE, as previously described.[11] Briefly, the cells were incubated with purified IgE (BD Biosciences) after blocking the Fcγ receptors with purified anti-CD16/32 antibody (BD Biosciences), stained with anti-IgE–fluorescein isothiocyanate (FITC; BD Biosciences), anti–Gr-1–phycoerythrin (PE), anti-Mac1–PE (eBioscience), and anti–c-Kit–allophycocyanin (APC; eBioscience), and then analyzed by FACSCalibur (BD Biosciences).

Peritoneal mast cells

Five milliliters ice-cold PBS was injected into the peritoneal cavity, and then 3 mL PBS was recovered. c-Kit and IgE receptor (FcεRI) expression was used to define the cells as peritoneal mast cells. Ly5.1 and Notch2 were stained with anti-Ly5.1–PE (BD Biosciences) or biotinylated anti-Notch2 antibody (clone HMN2-35)[8] followed by streptavidin PE (eBioscience), respectively.

Bone marrow transplantation

C57BL/6 mice and *W*^{sh}/*W*^{sh} mice were lethally irradiated with a total dose of 9.5 Gy and then transplanted with 1×10^7 whole bone marrow cells from either *N2*-MxcKO-Ly5.1 mice or *Notch2*$^{flox/flox}$-Ly5.1 mice from the tail vein. Tissues of transplanted mice were assessed at 3 to 4 months after transplantation. Donor-cell engraftment was assessed by fluorescence-activated cell sorting (FACS) analysis of peripheral blood, which was stained by anti-Ly5.2–FITC (BD Biosciences) and anti-Ly5.1–PE.

S venezuelensis infection

Mice were infected by subcutaneous injection of third-stage infective larvae of *Strongyloides venezuelensis*. The degree of infection was monitored by counting the number of eggs per gram of feces. Mast cells were counted and presented as the number per 10 villus crypt units. BMMCs were washed with PBS twice and then cultured with 10 ng/mL IL-4 and 10 ng/mL IL-10 for 3 days. These Th2-conditioned BMMCs were injected at day 3 and day 6 of experiments.[15] In contrast to the bone marrow transplantation, mice were not irradiated before BMMC injection.

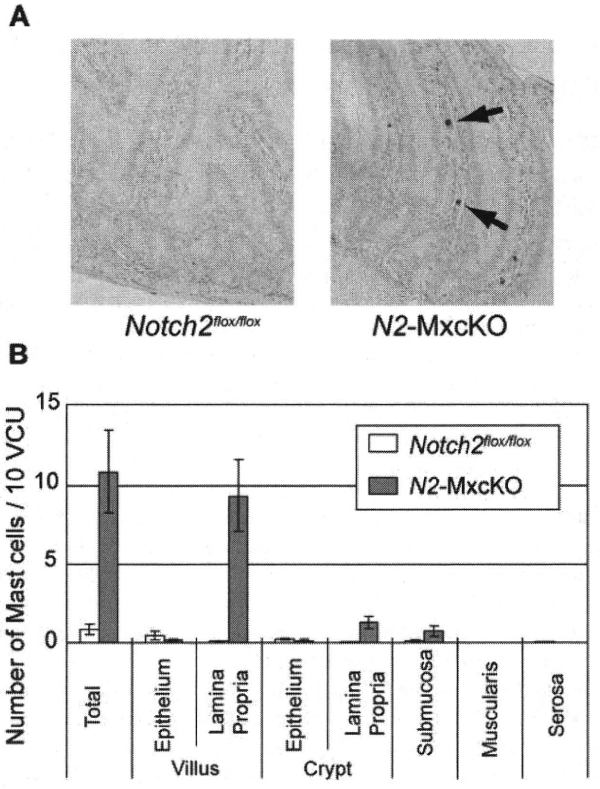

Figure 1. Mature mast cells were abnormally accumulated in the lamina propria of the small intestine of *Notch2*-deficient mice. (A) Sections of the small intestine of *N2*-MxcKO or littermate control *Notch2*$^{flox/flox}$ mice. Toluidine blue staining, followed by eosin. Original magnification ×200. (B) The numbers of mast cells per 10 villus crypt units (vcus) distributing to various layers of the small intestine. Data are presented as means ± SEM; *Notch2*$^{flox/flox}$ (n = 10) versus *N2*-MxcKO (n = 8); $P = .000461$ (total), $P = .000261$ (villus, lamina propria), $P = .001918$ (crypt, lamina propria), $P = .046874$ (submucosa).

Statistical analysis

The data for the number of mast cells and the *S venezuelensis* infection data were analyzed by the *t* test. *P* values < .05 were considered significant.

Results

Notch signaling affects the number and localization of mast cells in the small intestine

We have previously reported that Notch2 regulates mast cell differentiation in vitro.[11] To examine whether Notch2 controls the differentiation or development of MTMCs in vivo, we examined intestinal mast cells by toluidine blue staining in C57BL/6 mice carrying the *Notch2*$^{flox/flox}$ allele with or without the Mx1-*Cre* transgene (*N2*-MxcKO mice or *Notch2*$^{flox/flox}$ mice, respectively) after pIpC treatment.[13] Mast cells were only sparsely detected in the small intestine of *Notch2*$^{flox/flox}$ mice, mainly within the epithelium. However, the total number of mast cells in the small intestine of *N2*-MxcKO mice was unanticipatedly greater than that of *Notch2*$^{flox/flox}$ mice. Furthermore, those mast cells were mainly

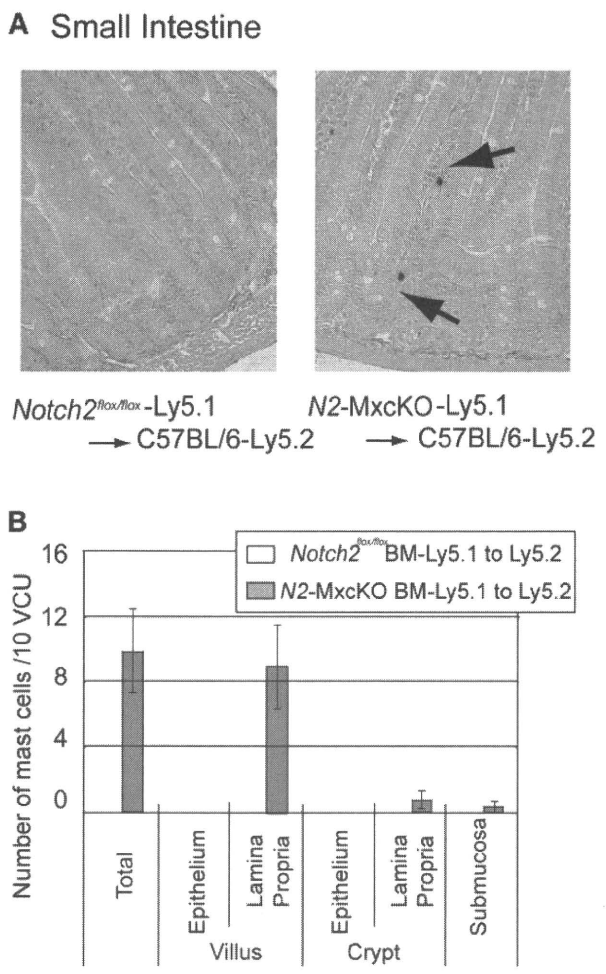

Figure 2. Localization of intestinal mast cells is abnormal in wild-type mice transplanted with *N2*-MxcKO-Ly5.1 bone marrow cells, reminiscent of that in *N2*-MxcKO mice. (A) Bone marrow cells from either *N2*-MxcKO- Ly5.1 mice or littermate *Notch2*$^{flox/flox}$- Ly5.1 mice were transplanted into lethally irradiated (9.5 Gy) C57BL/6-Ly5.2 mice. Toluidine blue staining, followed by eosin. Original magnification ×200. (B) The numbers of mast cells per 10 vcus distributing to various layers of the small intestine. Data are presented as means ± SEM; Mast cells in C57BL/6-Ly5.2 mice transplanted with *Notch2*$^{flox/flox}$-Ly5.1 (n = 3) versus *N2*-MxcKO-Ly5.1 (n = 3). $P = .020594$ (total) and $P = .030123$ (villus, lamina propria).

localized to the lamina propria, and very few mast cells were found within the epithelium (Figure 1A-B).

Localization of MTMCs is abnormal in wild-type mice transplanted with *N2*-MxcKO bone marrow cells, reminiscent of that in *N2*-MxcKO mice

Because the Mx-*Cre*–based conditional knockout system deletes target genes not only in the bone marrow cells but also, albeit partially, in the intestinal cells,[14] there was a possibility that *Notch2* deletion in the intestinal cells was responsible for the distinct distribution pattern or increased number of mast cells in *N2*-MxcKO mice compared with control mice. To exclude this possibility, we transplanted *Notch2*-null bone marrow cells carrying the Ly5.1 marker to irradiated wild-type C57BL/6-Ly5.2 mice. A chimerism of donor-derived Ly5.1-positive fraction accounted for more than 70% in the peripheral blood (data not shown). The recipients of bone marrow cells from *Notch2*$^{flox/flox}$ mice showed that the intestinal mast cell distribution was virtually the same as that in wild-type mice, whereas the recipients of *Notch2*-null bone marrow cells showed an increase in mast cells mainly in the lamina propria in an indistinguishable manner from the *N2*-MxcKO mice (Figure 2A-B). This result indicates that deletion of *Notch2* in bone marrow-derived cells alters the distribution pattern and increases the number of mast cells in the small intestine.

Notch-ligand expression in the small intestine

Notch signaling is known to be activated through Notch ligand-receptor binding.[16] We examined the expression pattern of Notch ligands in the small intestine with antibodies against Notch ligands Jagged1 and Delta1 and found that the epithelial layer was clearly stained with anti-Jagged1 but not with anti-Delta1 antibody (Figure 3). The staining with the anti-Jagged1 antibody was confined to the surface of epithelial cells, especially at their basal side rather than the apical side (Figure 3). The Jagged1 expression pattern suggests a possibility that Jagged1-Notch2 interaction between the basal side of the epithelial cells and mast cells has an important role for mast cell migration from the lamina propria across the basement membrane toward the epithelium (Figure 3). Furthermore, the ligand-receptor binding itself might contribute to mast cell–epithelial cell adhesion to some extent, based on our observation that *Notch2*-expressing BMMCs attached to the Jagged1-expressing Chinese hamster ovary (CHO) cells, while *Notch2*-null BMMCs did not (supplemental Figure 2).

Notch2 is dispensable for the CTMC development and distribution

We next investigated the roles of Notch2 in the development of CTMCs. The localization and the number of CTMCs in the skin and peritoneal cavity were not significantly different between *N2*-MxcKO and littermate *Notch2*$^{flox/flox}$ mice more than 4 weeks after the treatment with pIpC (data not shown). This observation might simply indicate that the Mx-*Cre* system was inefficient in the tissue-resident mast cells, as a great majority of peritoneal

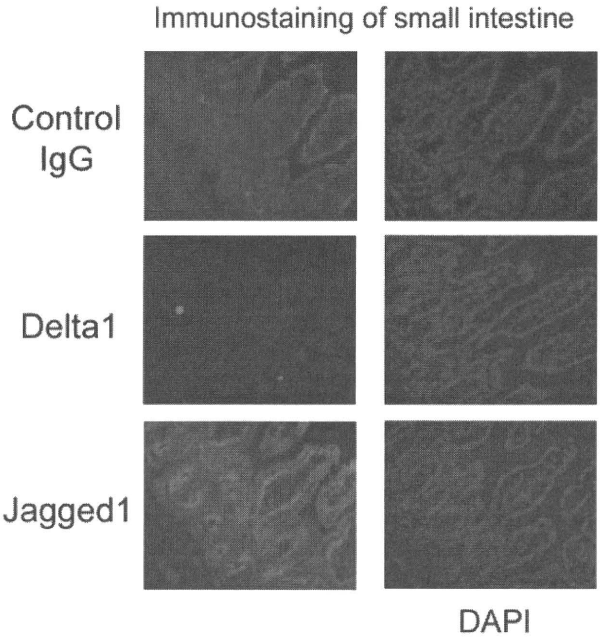

Figure 3. Jagged1 is strongly expressed on the surface of the epithelial cells, especially at their basal side. A section of small intestine prepared using cryostat was stained with goat anti-Jagged1 and goat anti-Delta1 antibodies followed by anti–goat Alexa594. Original magnification ×200.

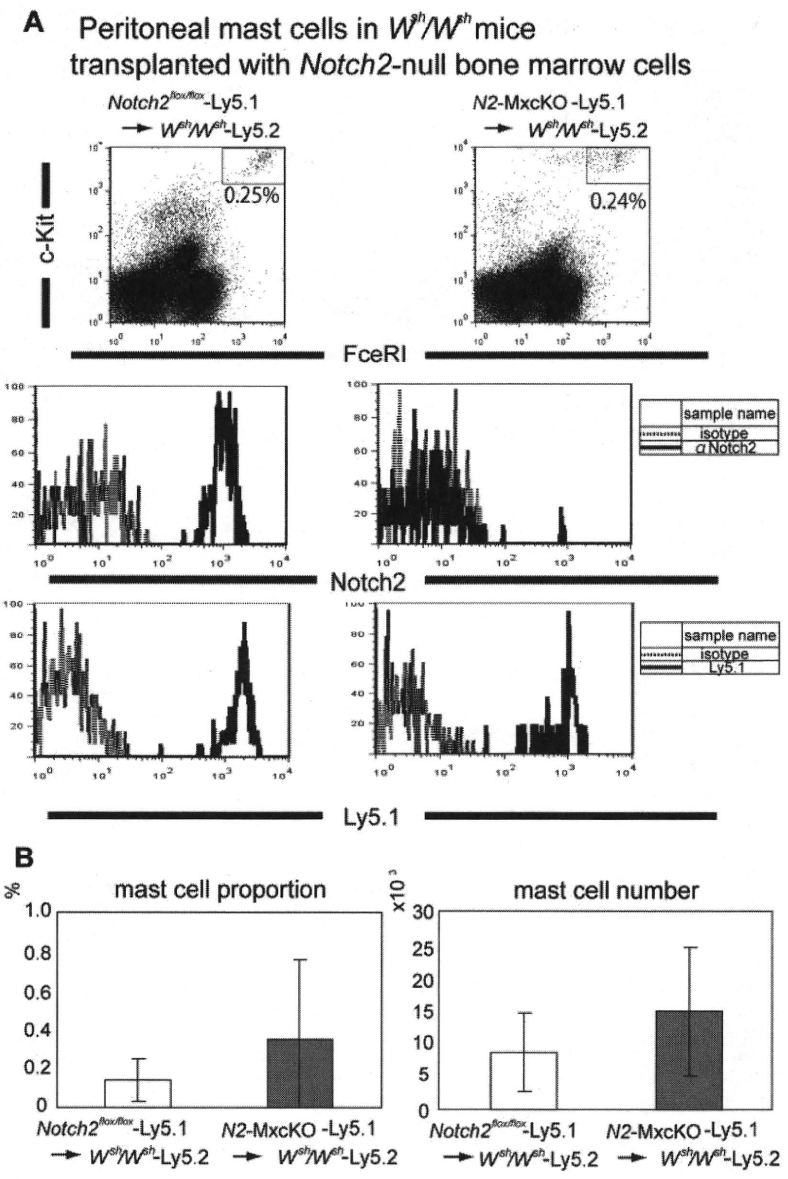

Figure 4. Notch2 is not required for peritoneal mast cell development. (A) Bone marrow cells from *N2*-MxcKO-Ly5.1 mice or control *Notch2*$^{flox/flox}$-Ly5.1 mice were transplanted into lethally irradiated *W*^{sh}/*W*^{sh} mice. Peritoneal mast cells were stained with anti–c-Kit–APC, IgE, and biotinylated anti-Notch2 antibody (HMN2-35), followed by anti-IgE–FITC and streptavidin-PE, or they were stained with anti–c-Kit–APC, IgE, and anti-Ly 5.1–PE, followed by anti-IgE–FITC; they were then analyzed by FACSCalibur (BD Biosciences). (B) The proportion (left) and the absolute number (right) of peritoneal mast cells were not significantly different between *W*^{sh}/*W*^{sh} mice transplanted with *Notch2*-WT bone marrow cells and those transplanted with *Notch2*-null bone marrow cells. $P = .210642$ (mast cell proportion) and $P = .196045$ (mast cell number).

mast cells of pIpC-treated *N2*-MxcKO mice still expressed Notch2 (data not shown). Therefore, to clarify the requirement of *Notch2* in the CTMC development, we examined peritoneal mast cells in mast cell-deficient *W*^{sh}/*W*^{sh} mice after transplantion of *Notch2*-null bone marrow cells carrying the Ly5.1 marker. In this system, mast cells exclusively develop from transplanted bone marrow progenitors, in which the *Cre* recombinase under the Mx-promoter is quite effective [14] (supplemental Figure 1). In this experiment, we found that the proportion and absolute number of peritoneal mast cells was not significantly different between those developed from the *N2*-MxcKO-Ly5.1 bone marrow cells and those developed from littermate *Notch2*$^{flox/flox}$-Ly5.1 bone marrow cells (Figure 4A-B). Notch2 was not expressed in the peritoneal mast cells derived from *N2*-MxcKO-Ly5.1 bone marrow cells but was expressed in those derived from littermate *Notch2*$^{flox/flox}$-Ly5.1 bone marrow cells (Figure 4A middle), indicating that *Notch2* was deleted efficiently. These results suggest that Notch2 is dispensable for the development and distribution of CTMCs.

Cell-autonomous Notch2 signaling in mast cells is important for mast cell migration across the basement membrane in the small intestine

We then asked a question whether aberrant mast cell migration in the small intestine in *N2*-MxcKO mice is dependent on Notch2 signaling in mast cells per se. We intravenously infused *Notch2*-null or control BMMCs into nonirradiated *W*^{sh}/*W*^{sh} mice after *S venezuelensis* infection, because it is reported that BMMCs could only transiently reconstitute intestinal mast cells in mast-cell deficient mice if these recipient mice are in naive status.[17] In tissue sections, we found that the distribution of mast cells in the small intestine was different between control BMMCs-reconstituted mice and *Notch2*-null BMMCs-reconstituted mice; control BMMCs were mainly migrated into the epithelial layer, while a majority of *Notch2*-null BMMCs remained in the lamina propria. This observation indicates that mast cell-autonomous Notch2 expression contributes to mast cell migration across the basement membrane from lamina propria into the epithelial layer (Figure 5A-B). Even in the control BMMC-infused mice, however, a substantial proportion of

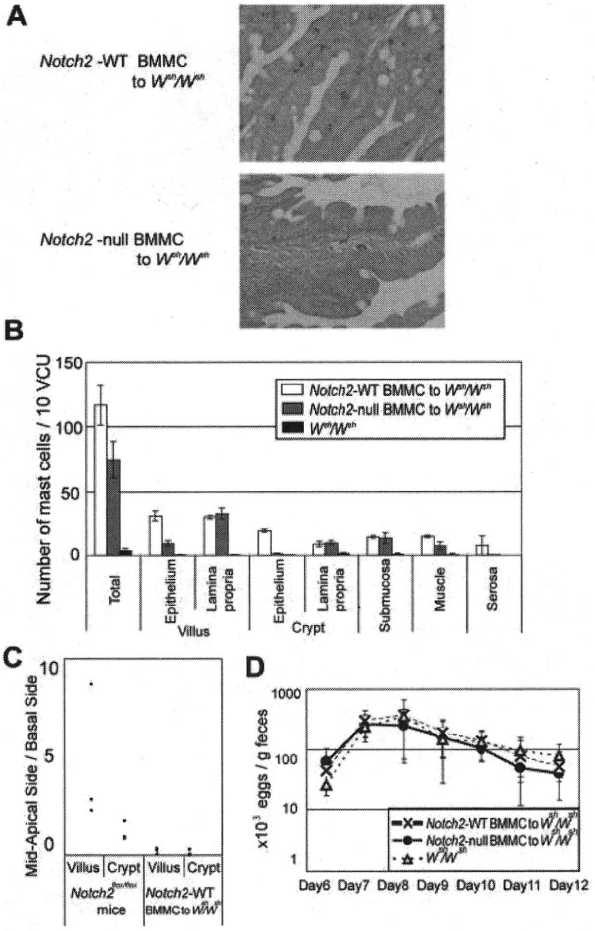

Figure 5. Mast cell–autonomous Notch2 expression is required for mast cell migration toward the epithelium. W^{sh}/W^{sh} mice infected with *S venezuelensis* were intravenously infused with Th2-conditioned *Notch2*-null or control BMMCs on days 3 and 6 of infection. (A) *Notch2*-null BMMCs poorly migrated toward the epithelium compared with control BMMCs. Toluidine blue staining followed by eosin staining. Original magnification ×200. (Top) Control BMMCs; (Bottom) *Notch2*-null BMMCs. (B) The number of mast cells per 10 vcus in the small intestine on day 12 after *S venezuelensis* infection in W^{sh}/W^{sh} mice, without BMMC infusion, with control BMMC infusion, and with *Notch2*-null BMMC infusion. Data are presented as means ± SEM; n = 3 (control BMMC infusion) and n = 4 (*Notch2*-null BMMC infusion), $P = .004080$ (villus, epithelium) and $P = .000020$ (crypt, epithelium). Note that mast cells in W^{sh}/W^{sh} mice infused with *Notch2*-null BMMCs abnormally resided in the lamina propria, whereas most of those in W^{sh}/W^{sh} mice infused with control BMMCs had intraepithelially migrated. (C) Mast cell number in mid to apical side of the epithelial layer was divided with that in the basal side of the epithelial layer. (D) Time course of *S venezuelensis* egg numbers in the stool. The number of excreted eggs was not significantly different between W^{sh}/W^{sh} mice infused with *Notch2*-null and control BMMCs. Data are presented as means ± SEM.

mast cells still remained in the lamina propria, submucosa, and smooth muscle layers, and the distribution of mast cells within the epithelium was confined to the basement membrane side of the epithelial layer (Figure 5B-C). This mast cell localization pattern was different from that in the $Notch2^{flox/flox}$ mice with *S venezuelensis* infection, in which mast cells were present mainly at the mid to apical side of the epithelial layer (Figure 5C). The numbers of *S venezuelensis* eggs in the stool were virtually the same in the *S venezuelensis*–infected W^{sh}/W^{sh} mice infused with *Notch2*-null and control BMMCs and in the *S venezuelensis*–infected W^{sh}/W^{sh} mice without any BMMC infusion throughout the period after infection (Figure 5D).

Taken together, the BMMC-W^{sh}/W^{sh} transplantation model demonstrated that Notch2 in the mast cells indeed determines their intraepithelial migration from lamina propria; nevertheless, this model was not adequate to examine the physiologic mast cell distribution pattern and subsequent parasite expulsion that depends on mast cells.

Notch2 signaling regulates antiparasite immunity of mast cells in the intestine

The BMMC-W^{sh}/W^{sh} reconstitution model could not completely reflect physiologic mast cell distribution pattern in the small intestine. Therefore, to further assess the effect of Notch2 signaling on the mucosal immune response of intestinal mast cells under a pathologic condition, *N2*-MxcKO or control $Notch2^{flox/flox}$ mice were infected with *S venezuelensis*. Total mast cell number was increased in $Notch2^{flox/flox}$ mice much more than in *N2*-MxcKO mice, especially in the epithelium in both crypts and villi 8 days after infection (Figure 6A-B). Thirteen days after infection, mast cells in the epithelium in $Notch2^{flox/flox}$ mice were still more abundant than those in *N2*-MxcKO mice (Figure 6C-D), while mast cell accumulation in the lamina propria in *N2*-MxcKO mice was more prominent in both villi and crypt than that in the earlier stage of infection (Figure 6A,C). In particular, dense aggregation of mast cells was prominent in the lamina propria of *N2*-MxcKO mice at the tip of the villi (Figure 6D). As a consequence, the total number of mast cells in the intestine of *N2*-MxcKO mice became equivalent to those of $Notch2^{flox/flox}$ mice 13 days after infection (Figure 6C,E). The number of *S venezuelensis* eggs in the stool was gradually decreased during day 8 to 10 in control $Notch2^{flox/flox}$ mice but not in *N2*-MxcKO mice (Figure 6F). Furthermore, the worms were still observed in *N2*-MxcKO mice but not in $Notch2^{flox/flox}$ mice 12 days after infection (Figure 6G). These data suggest that Notch2 deficiency alters the distinct distribution pattern of mast cells in the small intestine, which is responsible for the defective eradication of *S venezuelensis*.

Discussion

There is a growing body of evidence that Notch signaling modulates cellular migration and adhesion in endothelial, neural, and lymphoid lineage cells, as well as cancer cells.[18] We have shown that Notch2 signaling induces the development of mast cells.[11] However, it has remained unclear whether Notch2 signaling is involved in the distribution of mast cells in the intestinal mucosa or connective tissues or in controlling the functions of mast cells against microorganisms. Here, we investigated the role of Notch2 signaling in mast cells in terms of their distribution and functions using cell-specific *Notch2*-deficient mice. We found that in *N2*-MxcKO mice, mast cells were abnormally accumulated in the lamina propria of the small intestine, suggesting that *Notch2*-null mast cells have some defect in the migration toward the epithelium. Furthermore, *N2*-MxcKO mice failed to eradicate *S venezuelensis* and exhibited a distinct mast cell migration pattern in the intestine compared with control mice, suggesting that mast cells regulate the host-microbial interface in the intestine through Notch2 signaling.

Mast cell number was rather increased in the intestinal mucosa of *N2*-MxcKO mice compared with control mice in naive status. Mast cell progenitors were supposed to reside in the submucosa and gradually move toward the villi, accompanied by their differentiation into mature mast cells. Based on our observation in

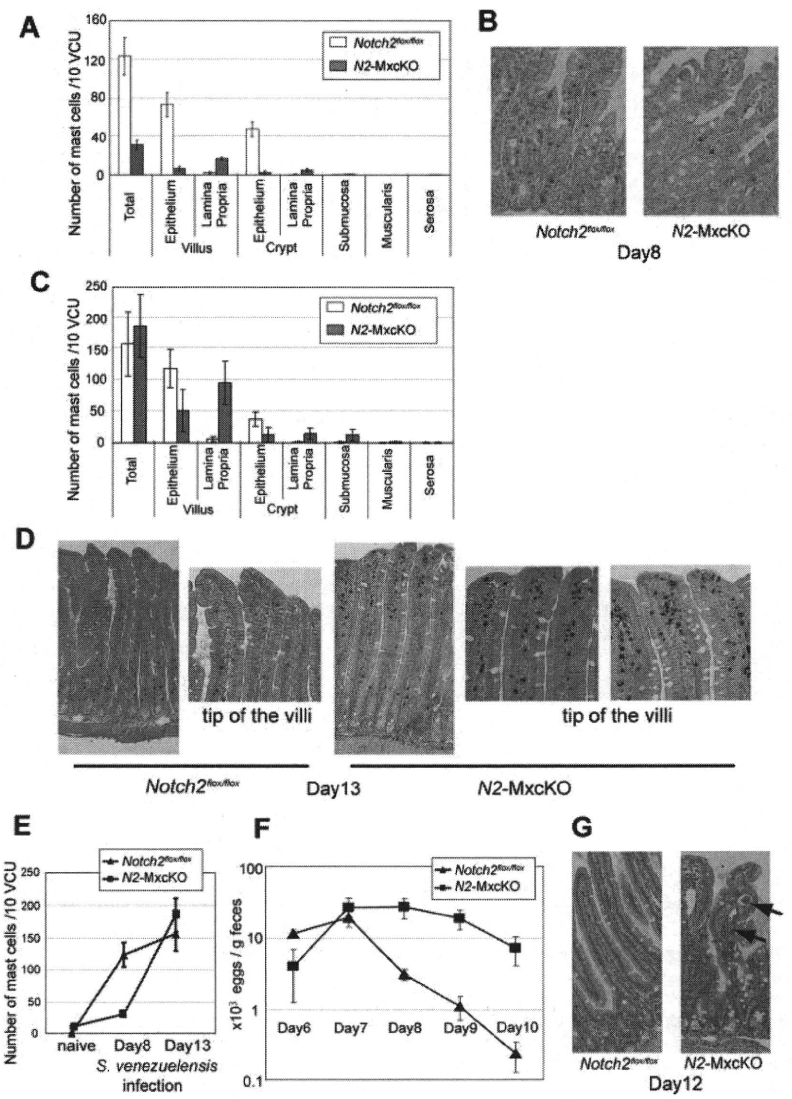

Figure 6. Notch2 is essential for antiparasite immunity of mast cells in the intestine. *N2*-MxcKO or control *Notch2*$^{flox/flox}$ mice were subcutaneously injected with third-stage infective larvae of *S venezuelensis*. (A) The number of mast cells per 10 vcus in the small intestine on day 8 after *S venezuelensis* infection. Data are presented as means ± SEM. The number of mast cells was much less in *N2*-MxcKO mice; n = 3, $P = .008592$ (total), $P = .005695$ (villus, epithelium), $P = .000715$ (villus, lamina propria), $P = .005245$ (crypt, epithelium), and $P = .045466$ (crypt, lamina propria). Note that mast cells in *N2*-MxcKO mice were abnormally clustered in the lamina propria, whereas most of those in the control *Notch2*$^{flox/flox}$ mice were intraepithelially migrated. (B) Toluidine blue staining followed by eosin staining of the small intestine on day 8; original magnification ×200. (C) The number of mast cells per 10 vcus in the small intestine on day 13 after *S venezuelensis* infection. Data are presented as means ± SEM; n = 3, $P = .026076$ (villus, epithelium), $P = .00194$ (villus, lamina propria), $P = .021177$ (crypt, epithelium), and $P = .019324$ (crypt, lamina propria), $P = .047445$ (submucosa). (D) Toluidine blue staining followed by eosin staining of the small intestine on day 13. Original magnification ×200. (E) The total number of mast cells per 10 vcus on day 0, day 8, and day 13 of infection. The total number of mast cells was significantly lower in *N2*-MxcKO mice at the early phase (day 8) and almost equal at the later phase (day 13) to that of control mice. Data are presented as means ± SEM; n = 10 and 8 (day 0, *Notch2*$^{flox/flox}$ and *N2*-MxcKO); n = 3 and 3 (day 8, *Notch2*$^{flox/flox}$ and *N2*-MxcKO); n = 4 and 4 (day 13, *Notch2*$^{flox/flox}$ and *N2*-MxcKO). (F) Time course of egg number in the stool. The number of excreted eggs was significantly greater in *N2*-MxcKO mice compared with those in *Notch2*$^{flox/flox}$ mice. Data are represented as means ± SEM; n = 4; $P = .0291$ (day 8) and $P = .0219$ (day 9). (G) Hematoxylin-eosin staining of the small intestine on day 12. Original magnification ×200. Arrows indicate worms. Worms were still observed in the villi in the jejunum of *N2*-MxcKO, but not of *Notch2*$^{flox/flox}$ mice.

an *S venezuelensis*–infection model, mast cells increase in number in the epithelium in control *Notch2*$^{flox/flox}$ mice, while they abnormally aggregate in lamina propria in *N2*-MxcKO mice, especially in the later stage of infection. This suggests that mast cell migration from lamina propria toward the epithelium across the basement membrane is impaired in *N2*-MxcKO mice. Consequently, mast cell turnover might be prolonged in *N2*-MxcKO mice. Given that the mechanism of mast cell migration from lamina propria toward the epithelium is common in naive status and infection status, such migration defect may also explain the mast cell increase in *N2*-MxcKO mice in naive status that we observed.

The defect of mast cell migration toward intraepithelium of the small intestine in *N2*-MxcKO mice is very similar to that in integrin β6-deficient mice,[19] in which activation of transforming growth factor (TGF)–β signaling is impaired.[20] A crosstalk between Notch signaling and TGF-β signaling might occur in intestinal mast cells as well as the cases of other cell types.[21] Alternatively, Notch signaling might directly regulate a downstream target of TGF-β1 in intestinal mast cell migration (eg, the induction of integrin αE expression).[19,22] Integrin αE, forming an integrin αEβ7 complex on mast cells, binds to E-cadherin on epithelial cells and is involved in mast cell localization in the epithelium.[22] The expression level of integrin αEβ7, measured by flow cytometric analysis, however, was not affected by Notch-ligand stimulation in BMMCs (unpublished data).

In the previous paper we showed that Notch signaling facilitates mast cell lineage development at the expense of granulocyte/macrophage development from both common myeloid progenitors (CMPs) and granulocyte-macrophage progenitors (GMPs) in vitro.[11] Mast cells, however, were not depleted in *N2*-MxcKO mice in naive status in vivo, but rather slightly increased in the small intestine of *N2*-MxcKO mice. This clearly indicates that Notch2 signaling is dispensable for steady-state mast cell generation in vivo. However, the dynamic increase of mast cells during the early phase of intestinal parasite infection was markedly impaired in *N2*-MxcKO mice. The mechanisms underlying the Notch2 signaling requirement only in parasite-infected mice remain to be clarified. Nevertheless, rapidly increasing intestinal mast cells have to be supplied by mast cell progenitors. The pathways and mechanisms responsible for mast cell progenitor recruitment and trafficking are likely to be dynamic and susceptible to modification during inflammation.[1] Such a modulation of the mast cell generation pathway during intestinal infection might underlie the requirement of *Notch2* only during parasite infection. This is similar to

IL-3–deficient mice. IL-3 is essential for mast cell differentiation in vitro; however, IL-3–deficient mice have the normal number of mast cells at the steady state, whereas mast cell hyperplasia is impaired upon intestinal parasite infection.[23]

Our data showed that parasite expulsion was impaired in *N2*-MxcKO mice. We could not exclude the possibility that the *Notch2* deletion in immune cells other than mast cells modulate the response against the nematode infection. If we could show that Th2-conditioned wild-type BMMCs successfully eradicate *S venezuelensis* in W^{sh}/W^{sh} mice and that *Notch2*-null BMMCs do not, it would be clearer that Notch2 signaling in mast cells per se but not in other immune cells should be critically important for defense against *S venezuelensis* infection. The failure of rescue experiments may be caused by the abnormal mast cell distribution pattern of wild-type BMMCs in W^{sh}/W^{sh} mice. Nevertheless, the result of this experiment supported the previous finding that the proper epithelial migration of mast cells is required for efficient expulsion of *S venezuelensis*[24] and thus provides an insight that the impaired *S venezuelensis* expulsion in *N2*-MxcKO mice is attributed to the mast cell-autonomous deletion of *Notch2*.

In conclusion, our data clearly indicate that Notch2 receptor signaling is specifically required for proper intestinal mast cell distribution in a cell-autonomous manner. Furthermore, involvement of Notch2 signaling in mucosal immunity was proven, particularly for eradication of infected parasites, although whether this is due to the Notch2 signaling in mast cells is yet to be elucidated.

Acknowledgments

We thank Dr Shigeo Koyasu for kind advice on the parasite infection experiment and Dr Cliff Takemoto, Dr Eichi Morii, and Dr Keisuke Oboki for kind advice on the histochemistry. We also thank Dr Hiromitsu Nakauchi for the Ly5.1 mice.

This work was supported in part by Grants-in-Aid for Scientific Research from the Japan Society for the Promotion of Science (KAKENHI #21790905 to M.S.-Y. and #18659276 to S.C.) and by grants from Mitsubishi Pharma Research Foundation and Takeda Science Foundation.

Authorship

Contribution: M.S.-Y. designed and performed the research, analyzed the data, and wrote the paper; T.S., Y. Miyake, and Y. Morishita performed the research; T.I.S., H.M., and H.Y. contributed new reagents; E.N.-Y., K.K., M.F., S.O., and M.K. provided vital discussion; K.Y. designed the research; and S.C. designed the research, analyzed the data, and wrote the paper.

Conflict-of-interest disclosure: The authors declare no competing financial interests.

Correspondence: Shigeru Chiba, Department of Clinical and Experimental Hematology, University of Tsukuba, 1-1-1 Tennodai, Tsukuba, Ibaraki, 305-8575, Japan; e-mail: schiba-tky@umin.net.

References

1. Gurish MF, Boyce JA. Mast cells: ontogeny, homing, and recruitment of a unique innate effector cell. *J Allergy Clin Immunol.* 2006;117(6):1285-1291.
2. Galli SJ, Nakae S, Tsai M. Mast cells in the development of adaptive immune responses. *Nat Immunol.* 2005;6(2):135-142.
3. Maruyama H, Yabu Y, Yoshida A, Nawa Y, Ohta N. A role of mast cell glycosaminoglycans for the immunological expulsion of intestinal nematode, Strongyloides venezuelensis. *J Immunol.* 2000; 164(7):3749-3754.
4. Friend DS, Ghildyal N, Gurish MF, et al. Reversible expression of tryptases and chymases in the jejunal mast cells of mice infected with Trichinella spiralis. *J Immunol.* 1998;160(11):5537-5545.
5. Miller HR, Pemberton AD. Tissue-specific expression of mast cell granule serine proteinases and their role in inflammation in the lung and gut. *Immunology.* 2002;105(4):375-390.
6. Tsukumo S, Yasutomo K. Notch governing mature T-cell differentiation. *J Immunol.* 2004; 173(12):7109-7113.
7. Radtke F, Wilson A, Mancini SJ, MacDonald HR. Notch regulation of lymphocyte development and function. *Nat Immunol.* 2004;5(3):247-253.
8. Maekawa Y, Minato Y, Ishifune C, et al. Notch2 integrates signaling by the transcription factors RBP-J and CREB1 to promote T-cell cytotoxicity. *Nat Immunol.* 2008;9(10):1140-1147.
9. Singh N, Phillips RA, Iscove NN, Egan SE. Expression of notch receptors, notch ligands, and fringe genes in hematopoiesis. *Exp Hematol.* 2000;28(5):527-534.
10. Jonsson JI, Xiang Z, Pettersson M, Lardelli M, Nilsson G. Distinct and regulated expression of Notch receptors in hematopoietic lineages and during myeloid differentiation. *Eur J Immunol.* 2001;31(11):3240-3247.
11. Sakata-Yanagimoto M, Nakagami-Yamaguchi E, Saito T, et al. Coordinated regulation of transcription factors through Notch2 is an important mediator of mast cell fate. *Proc Natl Acad Sci U S A.* 2008;105(22):7839-7844.
12. Nakano N, Nishiyama C, Yagita H, et al. Notch signaling confers antigen-presenting cell functions on mast cells. *J Allergy Clin Immunol.* 2009; 123(1):74-81 e71.
13. Saito T, Chiba S, Ichikawa M, et al. Notch2 is preferentially expressed in mature B cells and indispensable for marginal zone B lineage development. *Immunity.* 2003;18(5):675-685.
14. Kuhn R, Schwenk F, Aguet M, Rajewsky K. Inducible gene targeting in mice. *Science.* 1995; 269(5229):1427-1429.
15. Fukao T, Yamada T, Tanabe M, et al. Selective loss of gastrointestinal mast cells and impaired immunity in PI3K-deficient mice. *Nat Immunol.* 2002;3(3):295-304.
16. Kopan R, Ilagan MX. The canonical Notch signaling pathway: unfolding the activation mechanism. *Cell.* 2009;137(2):216-233.
17. Tanzola MB, Robbie-Ryan M, Gutekunst CA, Brown MA. Mast cells exert effects outside the central nervous system to influence experimental allergic encephalomyelitis disease course. *J Immunol.* 2003;171(8):4385-4391.
18. Nam DH, Jeon HM, Kim S, et al. Activation of notch signaling in a xenograft model of brain metastasis. *Clin Cancer Res.* 2008;14(13):4059-4066.
19. Brown JK, Knight PA, Pemberton AD, et al. Expression of integrin-alphaE by mucosal mast cells in the intestinal epithelium and its absence in nematode-infected mice lacking the transforming growth factor-beta1-activating integrin alphav-beta6. *Am J Pathol.* 2004;165(1):95-106.
20. Munger JS, Huang X, Kawakatsu H, et al. The integrin alpha v beta 6 binds and activates latent TGF beta 1: a mechanism for regulating pulmonary inflammation and fibrosis. *Cell.* 1999;96(3): 319-328.
21. Kluppel M, Wrana JL. Turning it up a Notch: cross-talk between TGF beta and Notch signaling. *Bioessays.* 2005;27(2):115-118.
22. Wright SH, Brown J, Knight PA, Thornton EM, Kilshaw PJ, Miller HR. Transforming growth factor-beta1 mediates coexpression of the integrin subunit alphaE and the chymase mouse mast cell protease-1 during the early differentiation of bone marrow-derived mucosal mast cell homologues. *Clin Exp Allergy.* 2002;32(2):315-324.
23. Lantz CS, Boesiger J, Song CH, et al. Role for interleukin-3 in mast-cell and basophil development and in immunity to parasites. *Nature.* 1998; 392(6671):90-93.
24. Abe T, Nawa Y. Localization of mucosal mast cells in W/Wv mice after reconstitution with bone marrow cells or cultured mast cells, and its relation to the protective capacity to Strongyloides ratti infection. *Parasite Immunol.* 1987;9(4):477-485.

Hes1 immortalizes committed progenitors and plays a role in blast crisis transition in chronic myelogenous leukemia

Fumio Nakahara,[1-4] Mamiko Sakata-Yanagimoto,[1,2,5] Yukiko Komeno,[3,4] Naoko Kato,[3,4] Tomoyuki Uchida,[3,4] Kyoko Haraguchi,[1,6] Keiki Kumano,[1,2] Yuka Harada,[7] Hironori Harada,[8] Jiro Kitaura,[3,4] Seishi Ogawa,[9] Mineo Kurokawa,[1,2] Toshio Kitamura,[3,4] and Shigeru Chiba[1,5]

[1]Department of Cell Therapy and Transplantation Medicine and [2]Department of Hematology Oncology, University of Tokyo, Tokyo; [3]Division of Cellular Therapy, Advanced Clinical Research Center, University of Tokyo, Tokyo; [4]Division of Stem Cell Signaling, Center for Stem Cell Therapy, Institute of Medical Science, University of Tokyo, Tokyo; [5]Department of Clinical and Experimental Hematology, Graduate School of Comprehensive Human Sciences, University of Tsukuba, Ibaraki; [6]Division of Transfusion and Cell Therapy, Tokyo Metropolitan Cancer and Infectious Disease Center Komagome Hospital, Tokyo; [7]International Radiation Information Center, Hiroshima University, Hiroshima; [8]Department of Hematology and Oncology, Research Institute for Radiation Biology and Medicine, Hiroshima University, Hiroshima; and [9]Cancer Genomics Project, Graduate School of Medicine, University of Tokyo, Tokyo, Japan

Hairy enhancer of split 1 (Hes1) is a basic helix-loop-helix transcriptional repressor that affects differentiation and often helps maintain cells in an immature state in various tissues. Here we show that retroviral expression of Hes1 immortalizes common myeloid progenitors (CMPs) and granulocyte-macrophage progenitors (GMPs) in the presence of interleukin-3, conferring permanent replating capability on these cells. Whereas these cells did not develop myeloproliferative neoplasms when intravenously administered to irradiated mice, the combination of Hes1 and BCR-ABL in CMPs and GMPs caused acute leukemia resembling blast crisis of chronic myelogenous leukemia (CML), resulting in rapid death of the recipient mice. On the other hand, BCR-ABL alone caused CML-like disease when expressed in c-Kit-positive, Sca-1-positive, and lineage-negative hematopoietic stem cells (KSLs), but not committed progenitors CMPs or GMPs, as previously reported. Leukemic cells derived from Hes1 and BCR-ABL-expressing CMPs and GMPs were more immature than those derived from BCR-ABL-expressing KSLs. Intriguingly, Hes1 was highly expressed in 8 of 20 patients with CML in blast crisis, but not in the chronic phase, and dominant negative Hes1 retarded the growth of some CML cell lines expressing Hes1. These results suggest that Hes1 is a key molecule in blast crisis transition in CML. (*Blood*. 2010;115(14):2872-2881)

Introduction

The balance between activator and repressor basic helix-loop-helix transcription factors is crucial for the proper timing of cellular differentiation and normal morphogenesis of various tissues.[1] During embryogenesis, the basic helix-loop-helix protein hairy enhancer of split 1 (Hes1), functioning downstream of the Notch receptor,[2,3] blocks differentiation of neural stem cells by antagonizing Mash1[4] and affects the cell-fate decision of pancreatobiliary epithelial progenitors.[5] In the adult hematopoietic system, Hes1 blocks granulocyte colony-stimulating factor-induced granulocytic differentiation of the 32D cell line,[6] preserving the long-term reconstituting ability of hematopoietic stem cells (HSCs) in vitro as well as in vivo.[7] Hes1 also plays a significant role in the development of perinatal T cells,[8,9] and knocking out Hes1 leads to lack of thymus.[9]

Recently, activating mutations of the *Notch1* and *Notch2* genes have been identified in more than 50% of human T-cell acute lymphoblastic leukemias[10] and in a subset of non-Hodgkin lymphomas,[11] respectively, implicating Notch signal deregulation based on a genetic abnormality in human cancers. The effect of Notch signal aberration, however, has been largely confined to lymphoid lineages in the hematopoietic compartment. Indeed, enhanced Notch signaling provides the bone-marrow-to-thymus transition stage of early progenitors, with strong selective pressure toward thymic T-cell precursors at the expense of B-cell and myeloid precursors.[12-14] We recently found that up-regulation of Hes1 represents only a part of Notch signaling during the decision between mast cell and granulocyte lineage differentiation. Notch signaling does promote mast-cell development at the expense of granulocyte differentiation through up-regulation of both Hes1 and GATA-3 in common myeloid progenitors (CMPs) and granulocyte-macrophage progenitors (GMPs). However, up-regulation of Hes1 alone causes expansion of cells with myeloid progenitor phenotypes, rather than mast cell development, mediated through down-regulation of a transcription factor, C-enhancer binding protein α (C/EBP-α).[15]

A growing volume of evidence shows that down-regulation of C/EBP-α represents major events in human acute myelogenous leukemia (AML), through either genetic or epigenetic abnormalities. Therefore, it is postulated that Hes1 up-regulation may be involved in a subset of myeloid leukemias.

Chronic myelogenous leukemia (CML) is a myeloproliferative neoplasm that originates in an abnormal pluripotent bone marrow stem cell and is consistently associated with the *BCR-ABL* fusion gene. The disease is biphasic or triphasic; an initial indolent chronic phase is followed by one or both of the aggressive stages, the accelerated phase and blast crisis, resulting in expansion of immature leukemic cells. The mainstay of chronic phase to blast

Submitted May 19, 2009; accepted September 27, 2009. Prepublished online as *Blood* First Edition paper, October 27, 2009; DOI 10.1182/blood-2009-05-222836.

The online version of this article contains a data supplement.

The publication costs of this article were defrayed in part by page charge payment. Therefore, and solely to indicate this fact, this article is hereby marked "advertisement" in accordance with 18 USC section 1734.

crisis transition is the differentiation block by additional genetic events in progenitor stages of CML cells[16] that could otherwise differentiate during the chronic phase. Thus, the transformation of BCR-ABL-induced myeloproliferative neoplasm to full-blown blast crisis has been drawing tremendous attention from investigators.

Here we show that retroviral expression of Hes1 immortalizes CMPs and GMPs in vitro. Hes1 introduction together with BCR-ABL into CMPs and GMPs, the postulated origin of blast crisis transition in CML, induced CML blast crisis-like disease when intravenously administered to sublethally irradiated mice. Considering as well the study of Hes1 expression in CML patients, we propose that Hes1 is a unique experimental tool for studying the mechanisms of chronic phase to blast crisis transformation in CML.

Methods

Mice

C57BL/6 (Ly5.1) donor mice were purchased from Sankyo Labo Service Corporation. C57BL/6 (Ly5.2) recipient mice were purchased from SLC. Mice were kept at the Animal Center for Biomedical Research, University of Tokyo, according to institutional guidelines.

Bone marrow progenitor sort

Bone marrow cells were isolated from the femurs and tibias of C57BL/6 (Ly5.1) donor mice (8-10 weeks of age) and were incubated with biotinylated antibodies for lineage markers, including anti-CD3, anti-CD4, anti-CD8, anti-B220, anti-Ter119, and anti–Gr-1 antibodies (BD Biosciences PharMingen) followed by incubation with streptavidin Micro Beads (Miltenyi Biotec). The lineage marker-negative (Lin^-) fraction was separated with an autoMACS separator or LS Columns (Miltenyi Biotec) and incubated with anti-CD34–fluorescein isothiocyanate, anti-CD16/32 (FcγRIII/II receptor)–phycoerythrin (PE), anti–c-Kit–allophycocyanin, streptavidin peridinin chlorophyll protein (BD Biosciences PharMingen), and anti–Sca-1–PE/Cy7 (eBioscience). Lin^-c-Kit^+Sca-1^+, Lin^-c-Kit^+Sca-1^-Fc$\gamma R^{lo}CD34^+$, and Lin^-c-Kit^+Sca-1^-Fc$\gamma R^{hi}CD34^+$ cells (KSLs, CMPs, and GMPs, respectively)[17] were sorted with a FACSAria cell sorter (BD Biosciences).

Transfection and retrovirus production for murine cells

Rat Hes1 cDNA, a gift from R. Kageyama (Kyoto University, Kyoto, Japan), was subcloned into a retrovirus vector, GCDNsam/internal ribosome entry site (IRES)–nerve growth factor receptor (NGFR), a gift from H. Nakauchi (University of Tokyo) and M. Onodera (National Center for Child Health and Development, Tokyo, Japan). BCR-ABL (p210) cDNA[18] was subcloned into a retrovirus vector, GCDNsam/IRES-GFP.[19] Mouse C/EBP-α cDNA, a gift from K. Akashi (Kyushu University, Fukuoka, Japan) and S. Mizuno (Dana-Farber Cancer Institute, Boston, MA), was subcloned into a retrovirus vector, pMYs-IRES-GFP.[19] Plat-E[20] packaging cells maintained in Dulbecco modified Eagle medium supplemented with 10% fetal calf serum were transfected with retroviral constructs using FuGENE 6 transfection reagent (Roche Diagnostics) according to the manufacturer's instructions. The medium was changed a day after transfection, and retroviruses were harvested 48 hours after transfection, as previously described.[19,20]

Transfection and retrovirus production for human cell lines

We generated a dominant-negative Hes1 (dnHes1) lacking a C-terminal WRPW (Trp-Arg-Pro-Trp) domain as described.[21] The fragment of dnHes1 was subcloned into pMYs-IRES-GFP.[19] Retrovirus packaging was done as described. Briefly, retroviruses were generated by transient transfection of Plat-A[20] packaging cells with FuGENE 6 (Roche Diagnostics).

Infection to progenitors

The retrovirus medium was placed in 24-well nontissue culture dishes for 4 hours at 37°C, precoated with 40 μg/mL of RetroNectin (Takara Bio) overnight at 4°C. After washing the wells with phosphate-buffered saline, sorted KSLs, CMPs, or GMPs were plated for infection for 48 to 60 hours with the coated retroviruses harboring GCDNsam/IRES-GFP-BCR-ABL (p210) or GCDNsam/IRES-NGFR-Hes1 or an empty vector as a control. Infection was done in StemSpan SFEM medium (StemCell Technologies) containing 100 ng/mL mouse stem cell factor (SCF), 100 ng/mL mouse thrombopoietin (TPO), and 100 ng/mL human FLT3 ligand (FL) for KSLs, or in Iscove modified Dulbecco medium (Sigma-Aldrich) containing 20% fetal calf serum, 50 ng/mL mouse SCF, 20 ng/mL mouse TPO, and 20 ng/mL mouse interleukin-3 (IL-3), 20 ng/mL human IL-6 (R&D Systems) for CMPs or GMPs.

Colony-forming assay

Retrovirus-infected cells were sorted at 48 to 60 hours from the initiation of infection with a FACSAria cell sorter (BD Biosciences) and used for colony-forming assay using Methocult 3231 (StemCell Technologies), supplemented with 50 ng/mL mouse SCF, 20 ng/mL mouse TPO, and 20 ng/mL mouse IL-3, 20 ng/mL human IL-6. A total of 1000 cells were cultured in each 2.5-cm dish in duplicate. The colony-forming cells were harvested and replated every 7 to 9 days and scored for colony formation. We defined a colony as "a group of cells, grown from a single parent cell, which is composed of more than 40 live cells."

Mouse bone marrow transplantation

Bone marrow cells prepared from C57BL/6-Ly5.1 mice were infected with retrovirus containing Hes1 or BCR-ABL, and 0.1 to 2.6×10^5 of Hes1/NGFR-sorted or BCR-ABL/GFP-sorted cells were injected through tail veins into C57BL/6-Ly5.2-recipient mice (8-12 weeks of age) after sublethal (5.25 Gy) or lethal (9.5 Gy) total body γ-irradiation (^{135}Cs). For the lethally irradiated mice, 2×10^5 of C57BL/6-Ly5.2 mice-derived bone marrow cells were simultaneously injected for radioprotection. Probabilities of overall survival of the mice that received transplantations were estimated using the Kaplan-Meier method. Statistical differences were determined by the Wilcoxon test. All animal studies were approved by the Animal Care Committee of the Institute of Medical Science, University of Tokyo.

Analysis of mice receiving transplantation

After transplantation, mice were monitored for signs of disease, such as cachexia, hyperpnea, or loss of gloss in fur. Autopsies were performed on moribund recipient mice. Peripheral blood count was analyzed by KX-21 Auto Analyzer (Sysmex). Morphology of the peripheral blood was evaluated by staining of air-dried smears with Hemacolor (Merck). Tissues including bone marrow, spleen, and liver were fixed in 10% buffered formalin, embedded in paraffin, sectioned, and stained with hematoxylin and eosin. Cytospin preparations of bone marrow and spleen cells were also stained with Hemacolor. Percentage of blasts, myelocytes, neutrophils, monocytes, lymphocytes, and erythroblasts was estimated by examination of at least 200 cells. To assess whether the leukemic cells were transplantable to secondary recipients, 0.1 to 5×10^6 total bone marrow cells were injected into the tail veins of sublethally irradiated mice. Two recipient mice were used for each serial transplantation.

Flow cytometric analysis

Red blood cells were lysed using Red Blood Cell Lysing Buffer (Sigma-Aldrich) in peripheral blood or single-cell suspensions of bone marrow and spleen. After washing with phosphate-buffered saline, Fc receptor was blocked by incubating cells with 2.4G2 antibody (eBioscience) for 15 minutes at 4°C and then staining them with the following PE-conjugated monoclonal antibodies for 20 minutes at 4°C: Ly-5.1, Gr-1, CD11b, B220, CD19, CD3, CD4, CD8, c-Kit, Sca-1, CD34, and Ter119. Flow-cytometric analysis of the stained cells was performed with FACSCalibur

(BD Biosciences) equipped with CellQuest software (BD Biosciences) and FlowJo software (TreeStar).

Patients

CML patients were diagnosed at Hiroshima University Hospital and its affiliated hospitals. Diagnosis was based on morphologic, immunophenotypic, and, in some cases, real-time reverse transcription-polymerase chain reaction (RT-PCR) studies according to the French-American-British classification or World Health Organization classification. Patient samples were prepared after the research plan was approved by the Institutional Review Board at Hiroshima University, and written informed consent was obtained in accordance with the Declaration of Helsinki. Investigations were carried out in accordance with ethical standards authorized by the ethics committee of Hiroshima University and the ethics committee of the University of Tokyo (approval no. 20-10-0620)

Real-time RT-PCR

Total RNA was extracted from human bone marrow or peripheral blood cells using a TRIzol Kit (Invitrogen) according to the manufacturer's instructions, and converted to cDNA with a High Capacity cDNA Reverse Transcription Kit (Applied Biosystems). Total RNA of mouse progenitors was extracted with RNeasy (QIAGEN) according to the manufacturer's instructions, and converted to cDNA with a High Capacity cDNA Reverse Transcription Kit (Applied Biosystems). Real-time RT-PCR was performed using a LightCycler Workflow System (Roche Diagnostics). cDNA was amplified using a SYBR Premix EX Taq (Takara). Reaction was subjected to 1 cycle of 95°C for 30 seconds, 45 cycles of PCR at 95°C for 5 seconds, 58°C for 10 seconds, and 72°C for 10 seconds. All samples were independently analyzed at least 3 times. The following primer pairs were used: 5′-CCAGTTTGCTTTCCTCATTCC-3′ (forward) and 5′-TCTTCTCTCCCAGTATTCAAGTTCC-3′ (reverse) for human Hes1[22]; 5′-GAGCTGAACGGGAAGCTCACTGG-3′ (forward) and 5′-CAACTGTGAGGAGGGGAGATTCAG-3′ (reverse) for human GAPDH[22]; 5′-GAACAGCAACGAGTACCGGGTA-3′ (forward) and 5′-CCCATGGCCTTGACCAAGGAG-3′ (reverse) for mouse C/EBP-α[23]; 5′-CACAGGACTAGAACACCTGC-3′ (forward) and 5′-GCTGGTGAAAAGGACCTCT-3′ (reverse) for mouse hypoxanthine phosphoribosyltransferase (HPRT).[23] Relative gene expression levels were calculated using standard curves generated by serial dilutions of cDNA. Product quality was checked by melting curve analysis via LightCycler software (Roche Diagnostics). Expression levels were normalized by a control, the expression level of GAPDH mRNA for human samples, and HPRT mRNA for mouse samples.

Western blot analysis

To detect the expression of Hes1 or BCR-ABL (p210) proteins, equal numbers of cells from spleen or cell line were lysed, and Western blotting was performed as described with minor modifications.[24] Polyclonal rabbit anti-Hes1 antibody (H-140; Santa Cruz Biotechnology) and polyclonal rabbit anti–c-ABL antibody (K-12; Santa Cruz Biotechnology) were used for Hes1 or BCR-ABL detection, respectively.

Results

Retroviral transduction of Hes1 immortalizes CMPs and GMPs

NGFR-sorted Hes1-transduced KSLs, CMPs, and GMPs similarly generated compact and relatively large colonies, whereas empty vector-transduced KSLs generated a similar number of less large colonies. Empty vector-transduced CMPs and GMPs did not generate colonies (Figure 1A). Cytospin preparations of Hes1-transduced progenitors, stained with Hemacolor (Merck), showed blast-like morphologies, whereas those of empty vector-transduced KSLs contained bands, macrophages, and blasts (Figure 1B). Most of the empty vector-transduced CMPs and GMPs died and few cells remained (Figure 1B). In serial colony-forming assays, both CMPs and GMPs transduced with Hes1 formed colonies after at least 4 rounds of replating, with the plating efficiency more than 15% at the fourth round (Figure 1C). Replating could be reproducibly maintained for more than half a year, implying immortalizing activity of Hes1 (Figure 1D). The Hes1-transduced KSLs, CMPs, and GMPs were dependent on the presence of IL-3, requiring concentrations more than 1 ng/mL (Figure 1E; supplemental Figure 1A-B, available on the *Blood* website; see the Supplemental Materials link at the top of the online article). There was no significant difference between these cells in the dependency on IL-3. The majority of Hes1-transduced cells expressed c-Kit and CD34 at high levels, Sca-1 and CD11b at intermediate levels (Figure 1F, supplemental Figure 2A-B), irrespective of whether they were derived from KSLs, CMPs, or GMPs (supplemental Figure 2E).

The Lin^- cells were further analyzed by adopting 5-color flow cytometry that is used to identify bone marrow KSLs, CMPs, and GMPs. The expression levels of c-Kit, Sca-1, and CD34 were distributed over wide ranges. Approximately 2.5% to 6.4% of all nucleated cells showed a phenotype similar to KSLs, and another 4.8% to 11.6% showed a phenotype similar to GMPs. There were few cells that resembled CMPs (Figure 1G). We sorted the KSL-like cells, CMP-like cells, and GMP-like cells from each Hes1-transduced cell (Hes1-KSLs, Hes1-CMPs, and Hes1-GMPs) and cultured them for a week in methylcellulose. The same analysis by 5-color flow cytometry showed accumulation of GMP-like cells (~ 45.3%-83.5% of all nucleated cells) and moderate accumulation of KSL-like cells (~ 4.3%-23.4% of all nucleated cells) in the cultured cells (supplemental Figure 3A-C).

BCR-ABL replaces IL-3 in Hes1-immortalized cell lines

Because the Hes1-immortalized cell lines were IL-3 dependent for their growth in vitro, we examined whether additional signaling could replace IL-3. IL-3 signaling takes place mainly via Stat-, Ras-MAPK-, and PI3K-Akt-dependent pathways. It is also known that CML-specific BCR-ABL (p210) can replace IL-3 signaling in several experimental designs. Thus, we retrovirally expressed BCR-ABL together with Hes1. The combination of Hes1 and BCR-ABL enabled KSLs, CMPs, and GMPs to form colonies after repeated replating, not only in the presence of cytokines (Figure 2A left panel) but also in the condition free from cytokines (Figure 2A right panel). In contrast, KSLs, but not CMPs or GMPs, formed colonies by BCR-ABL transduction alone only when supplemented with cytokines (Figure 2A left panel), and they did not form any colonies without cytokines (Figure 2A right panel) or after replating with/without cytokines (Figure 2A both panels). In the liquid culture, it was shown that KSLs, CMPs, and GMPs transduced with both Hes1 and BCR-ABL were immortalized without cytokine supplementation (Figure 2B). The colonies made from Hes1- and BCR-ABL-transduced cells showed similar morphology with those from Hes1-transduced cells in the presence of a cytokine cocktail (Figure 2C). Importantly, the morphology of colony-forming cells derived from BCR-ABL-transduced KSLs was much more mature compared with those derived from Hes1- and BCR-ABL-transduced KSLs, CMPs, and GMPs, even in the same cytokine cocktail (Figure 2D). The majority of $Hes1^+BCR\text{-}ABL^+$ KSLs as well as $Hes1^+BCR\text{-}ABL^+$ CMPs and GMPs expressed CD34 at high levels, whereas they expressed c-Kit, Sca-1, and CD11b at intermediate levels (Figure 2E; supplemental Figure 2C-D), irrespective of whether they were derived from

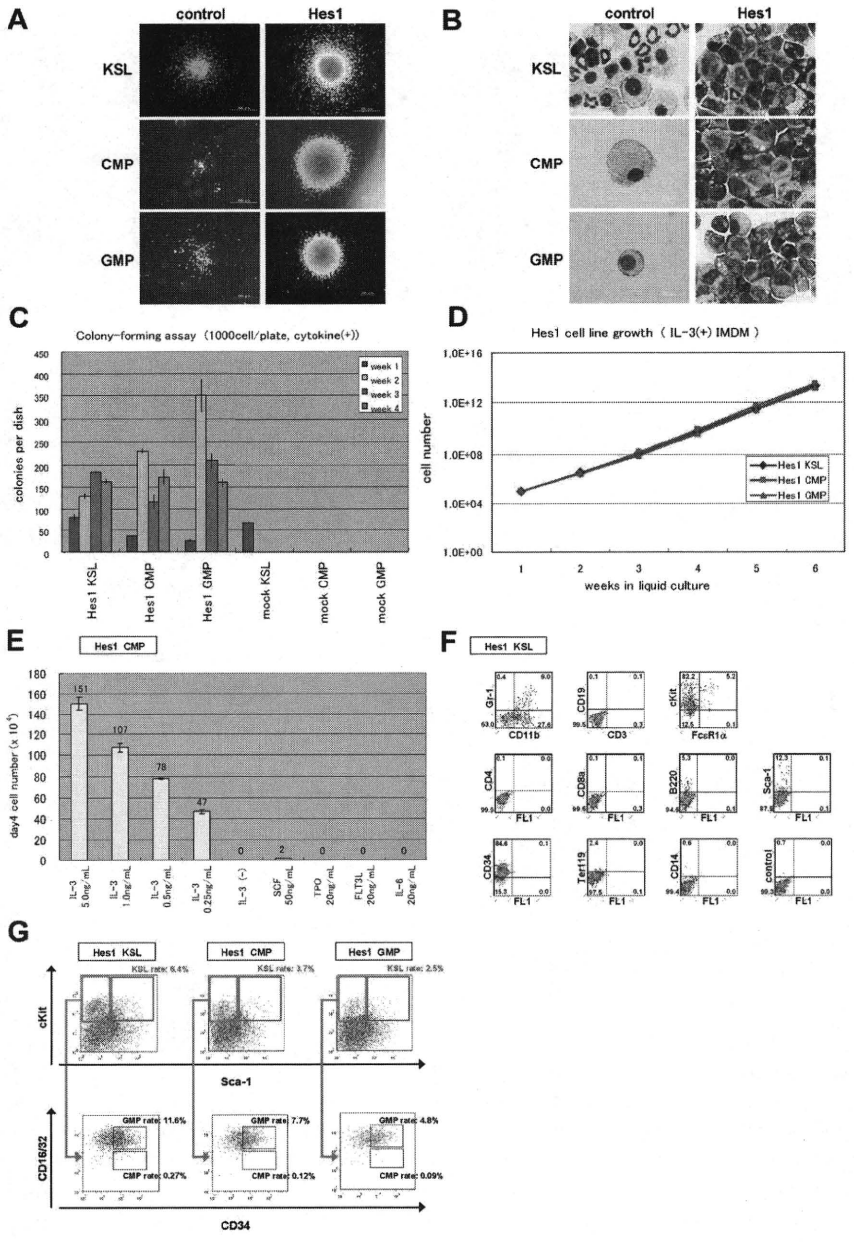

Figure 1. Hes1-transduced KSLs, CMPs, or GMPs were immortalized in the presence of IL-3. (A) Typical colonies derived from Hes1- and empty vector-transduced KSLs, CMPs, and GMPs in the presence of SCF, TPO, IL-3, and IL-6. Images were obtained with an IX70 microscope and a DP70 camera (Olympus); an objective lens, UPlanFI (Olympus); original magnification ×40 (bottom 2 in the right panels) and original magnification ×100 (remaining 4 panels). (B) Giemsa staining of Hes1- and control vector-transduced KSLs, CMPs, and GMPs. Images were obtained with a BX51 microscope and a DP12 camera (Olympus); an objective lens, UPlanFI (Olympus); original magnification ×1000. (C) Colony-forming assay from KSLs, CMPs, and GMPs transduced with Hes1 or empty vector. Hes1-transduced cells were replatable more than 4 times in vitro. Bars represent the number of colonies obtained per 10^3 cells after each round of plating in methylcellulose supplemented with SCF, TPO, IL-3, and IL-6. A representative result from 3 independent and reproducible experiments is shown. Error bars represent the SD from duplicate cultures. (D) Sustained growth of Hes1-transduced cells in liquid culture supplemented with 1 ng/mL IL-3. The number of cells was determined every 7 days by trypan blue staining, and 10^5 cells per well were seeded into a 6-well plate. Liquid culture was reproducibly continued for more than 6 months. (E) Cytokine requirement of Hes1-transduced CMPs. The cells were cultured in Iscove modified Dulbecco medium supplemented with indicated cytokines in duplicate. The numbers of cells were counted after 4 days of culture. A representative result from 2 independent and reproducible experiments is shown. Error bars represent the SD from duplicate cultures. Hes1-transduced KSLs and GMPs showed similar results (supplemental Figure 1A-B). (F) Flow-cytometric analysis of Hes1-transduced KSLs cultured in methylcellulose supplemented with SCF, TPO, IL-3, and IL-6. The dot plots represent Gr-1, CD19, c-Kit, CD4, CD8a, B220, Sca-1, CD34, Ter119, and CD14 labeled with a corresponding PE-conjugated monoclonal antibody versus CD11b, CD3, and FcεR1α labeled with a corresponding fluorescein isothiocyanate-conjugated monoclonal antibody or FL1 with no monoclonal antibody. Hes1-transduced CMPs and GMPs showed similar expression patterns (supplemental Figure 2A-B). (G) Flow-cytometric analysis of Lin^--gated Hes1-transduced cells. Five-color analyses are used to identify KSL-like (top panels) and CMP-like and GMP-like cells (bottom panels) in the Hes1-transduced KSLs, CMPs, and GMPs. The number shows the percentage of cells in all nucleated cells. The analyzed cells were NGFR sorted at 48 to 60 hours from the initiation of Hes1- or control vector-transduction and cultured for the following lengths of time before the analysis: (A) 1 week, (B) 1 week, (C) 0 days, (D) 4 weeks, (E) 2 weeks, (F) 1 week, and (E) 2 weeks.

KSLs, CMPs, or GMPs (supplemental Figure 2F). $Hes1^+BCR\text{-}ABL^+$ KSLs, CMPs, and GMPs showed lower expressions of c-Kit and CD34 than KSLs, CMPs, and GMPs transduced with Hes1 alone (supplemental Figure 2E-F) when cultured in the presence of the same cytokine cocktail (SCF, TPO, IL-3, and IL-6). Expression of Hes1 or BCR-ABL in the Hes1 ± BCR-ABL transduced CMP or GMP cell lines was confirmed by Western blot analysis (supplemental Figure 4A).

$Hes1^+BCR\text{-}ABL^+$ CMPs and GMPs rapidly induce AML/CML blast crisis-like disease in recipient mice

To examine the effect of Hes1 on leukemogenesis, Hes1-transduced KSLs, CMPs, and GMPs were injected through tail veins into C57BL/6-Ly5.2 recipient mice (8-12 weeks of age) after a sublethal (5.25 Gy) or a lethal (9.5 Gy) dose of total-body γ-irradiation (^{135}Cs). For the lethally irradiated mice, 2×10^5 bone marrow cells from C57BL/6-Ly5.2 mice were simultaneously injected for radioprotection. All the mice that received transplantations of Hes1-transduced KSLs, CMPs, and GMPs were kept healthy, and no recipients developed myeloproliferative neoplasms (MPNs) or leukemias for up to 250 days after the transplantation (Figure 3A). Regarding the nonleukemogenic nature of the stem/progenitor cells transduced with Hes1 alone, we[7] and others[25] previously reported similar results, although the cell populations and/or experimental designs were not identical.

In agreement with the previous reports,[26] recipient mice injected with BCR-ABL-transduced KSLs developed fatal MPN within 30 days after the transplantation, whereas those injected with BCR-ABL-transduced CMPs and GMPs were kept healthy for more than 130 days. We did not find any signs of MPN or leukemias when mice were killed between 130 and 200 days after the transplantation (Figure 3B).

Because we found that the combination of Hes1 and BCR-ABL transduction conferred cytokine-independent immortalization on CMPs and GMPs, we injected $Hes1^+BCR\text{-}ABL^+$ KSLs, CMPs, and GMPs through tail veins into C57BL/6-Ly5.2 recipient mice

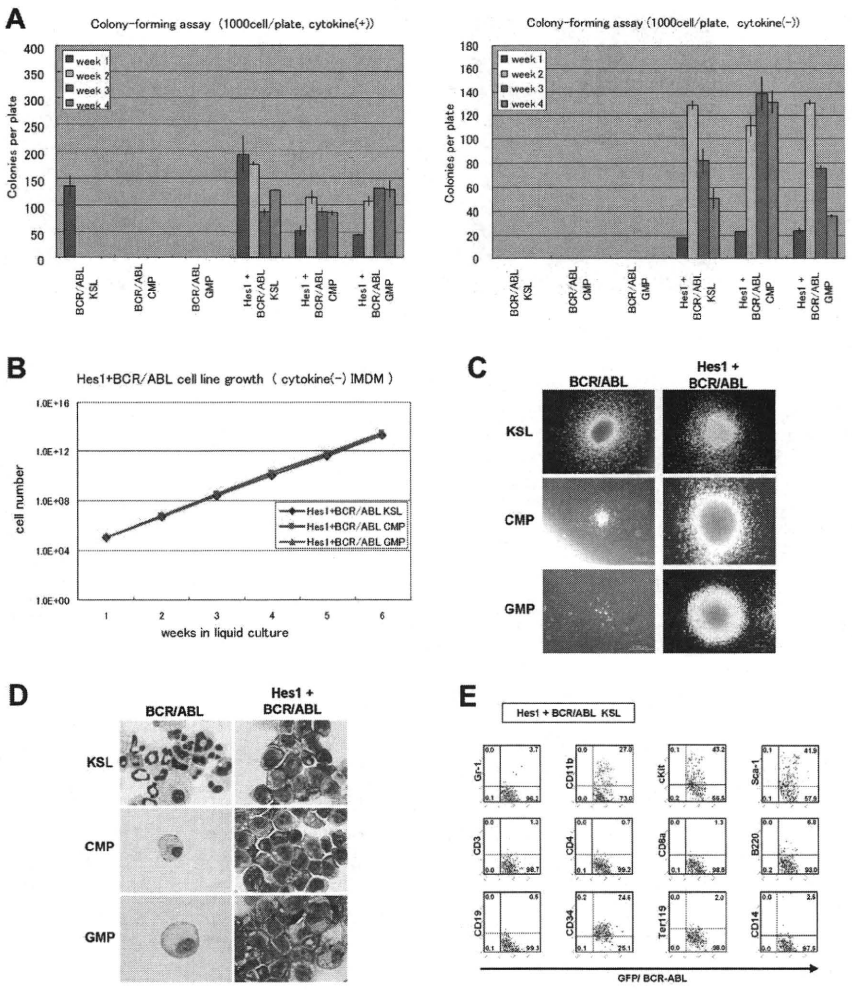

Figure 2. Hes1- and BCR-ABL-transduced KSLs, CMPs, or GMPs were immortalized independently of IL-3. (A) Colony-forming assay of KSLs, CMPs, and GMPs transduced with BCR-ABL alone or Hes1 and BCR-ABL, cultured in methylcellulose with or without cytokine cocktail containing SCF, TPO, IL-3, and IL-6. Hes1$^+$BCR-ABL$^+$ cells could be serially replated more than 4 times both with or without cytokines. In contrast, whereas KSLs, but not CMPs or GMPs, transduced with BCR-ABL alone, formed colonies in the presence of cytokines, neither KSLs, nor CMPs, nor GMPs formed colonies without cytokine supplementation. Bars represent the number of colonies obtained per 10^3 cells after each round of plating in methylcellulose. A representative result from 3 independent and reproducible experiments is shown. Error bars represent the SD from duplicate cultures. (B) Sustained growth of Hes1$^+$BCR-ABL$^+$ cells in liquid culture without cytokine supplementation. The numbers of cells were determined every 7 days by trypan blue staining, and 10^5 cells per well were seeded into a 6-well plate. Liquid culture was reproducibly continued for more than 6 months. (C) Typical colonies derived from KSLs, CMPs, and GMPs transduced with BCR-ABL alone (left panels) or BCR-ABL and Hes1 (right panels) in the presence of SCF, TPO, IL-3, and IL-6. Images were obtained with an IX70 microscope and a DP70 camera (Olympus); an objective lens, UPlanFl (Olympus); original magnification ×100. (D) Giemsa staining of Hes1$^+$BCR-ABL$^+$ KSLs, CMPs, and GMPs. Images were obtained with a BX51 microscope and a DP12 camera (Olympus); an objective lens, UPlanFl (Olympus); original magnification ×1000. (E) Flow-cytometric analysis of Hes1$^+$BCR-ABL$^+$ KSLs cultured in methylcellulose supplemented with SCF, TPO, IL-3, and IL-6. The dot plots represent Gr-1, CD11b, c-Kit, Sca-1, CD3, CD4, CD8a, B220, CD19, CD34, Ter119, and CD14 labeled with a corresponding PE-conjugated monoclonal antibody versus expression of GFP/BCR-ABL. Hes1$^+$BCR-ABL$^+$ CMPs and GMPs showed a similar expression pattern (supplemental Figure 2C-D). The analyzed cells were GFP and NGFR sorted at 48 to 60 hours from the initiation of BCR-ABL- or Hes1+BCR-ABL transduction and cultured for the following lengths of time before the analysis: (A) 0 days, (B) 4 weeks, (C) 1 week, (D) 1 week, and (E) 1 week.

after sublethal irradiation. The numbers of cells injected varied among experiments, ranging from 17×10^2 to 15×10^4, because of the difference in sorting efficiencies. All the mice receiving transplantations rapidly developed fatal AML/CML in blast crisis-like disease with no significant difference in latency, ranging between 18 and 39 days after the transplantation ($P < .867$) (Figure 4A). The tissue distribution of the disease was virtually the same among mice receiving KSLs, CMPs, and GMPs; they invariably demonstrated marked hepatosplenomegaly and lung hemorrhage resulting from infiltration of leukemic cells (Figure 4B). Expression of Hes1 and BCR-ABL in the spleen cells of recipient mice was confirmed by Western blot analysis (supplemental Figure 4B).

The morphology of bone marrow demonstrated increased myeloid blasts (Figure 4C), and the histology of spleen, liver, and lungs demonstrated extensive infiltration of leukemic cells (Figure 4D). The percentages of the blasts ranged between 28% and 55% of all nucleated bone marrow cells (mean, 36.5%) of the mice receiving Hes1- and BCR-ABL-transduced KSLs, CMPs, and GMPs. In contrast, the percentages of bone marrow blasts in the recipient mice receiving BCR-ABL-transduced KSLs were only 6% to 7% (Figure 5A). White blood cell counts in the peripheral blood of recipients with Hes1$^+$BCR-ABL$^+$ KSLs, CMPs, and GMPs were $2.4 \times 10^4/\mu L$ to $67.9 \times 10^4/\mu L$ (mean, $17.8 \times 10^4/\mu L$), whereas those with BCR-ABL-transduced KSLs showed moderate leukocytosis ranging between $2.9 \times 10^4/\mu L$ and $3.8 \times 10^4/\mu L$ (Figure 5B). The surface marker profiles of the bone marrow cells from the recipients with Hes1$^+$BCR-ABL$^+$ cells expressed CD11b and Gr-1 at high levels, whereas they expressed c-Kit, Sca-1, and CD34 at intermediate levels (Figure 5C; supplemental Figure 5A-B), irrespective of whether they were derived from KSLs, CMPs, or GMPs (supplemental Figure 5C).

The long-term self-renewal properties of the leukemic cells derived from Hes1- and BCR-ABL-transduced CMPs or GMPs were tested by transplantation into secondary recipients; 0.1 to 5×10^6 total bone marrow cells were injected into the tail veins of sublethally irradiated mice. All recipient mice transplanted with more than 10^5 Hes1$^+$ cells from bone marrow developed fatal AML/CML in blast crisis-like disease with latencies of between 18 and 75 days (supplemental Figure 4C). The disease was almost identical with the primary disease (data not shown).

Hes1 expression is elevated in a substantial subset of human CML blast crisis samples

The results presented from the mouse model experiments suggest a potential link between deregulated expression of Hes1 and human CML in blast crisis. We measured the Hes1 mRNA by real-time RT-PCR in 11 peripheral blood, 1 cerebrospinal fluid, and 8 bone marrow samples from CML in blast crisis patients; 19 bone marrow samples from CML in chronic phase patients; and 10 bone marrow samples from normal subjects. In 8 of 20 CML in blast crisis samples, we found that Hes1 mRNA levels were elevated by more than 4 times the average of normal bone marrow samples (Figure

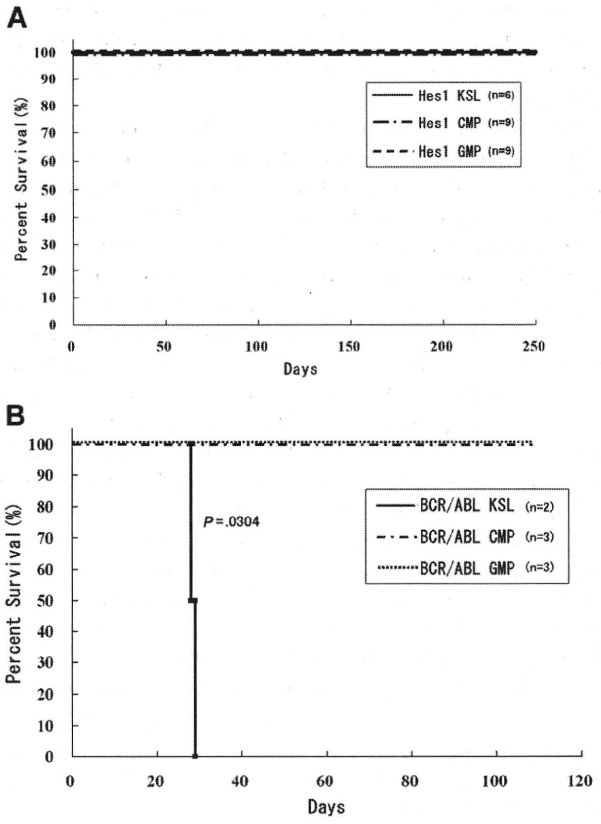

Figure 3. Mice transplanted with Hes1-transduced KSLs, CMPs, and GMPs were kept healthy. (A) Survival curves for mice injected with Hes1-transduced progenitors. No mice showed any signs of MPN for more than 250 days from transplantation. Data were analyzed by the Kaplan-Meier method. The numbers of transplanted mice are shown. Three independent experiments were performed. (B) Survival curves for mice injected with BCR-ABL-transduced progenitors. Mice transplanted with BCR-ABL-transduced KSLs developed fatal MPN within 30 days after transplantation, whereas mice transplanted with BCR-ABL-transduced CMPs or GMPs showed no evidence of disease when killed between 130 and 200 days after transplantation. Data were analyzed using the log-rank test. The 2 independent experiments were performed, and the total numbers of transplanted mice are shown.

6A). Interestingly, all but one of their phenotypes were myeloid, and 5 of 12 samples in which Hes1 mRNA levels were not elevated were derived from patients with B-cell lineage lymphoid crisis. On the other hand, the average of Hes1 mRNA levels in CML in chronic phase samples seemed to be lower than that of the normal bone marrow samples, with no sample exceeding twice the average. Clinical data of 20 patients with CML in blast crisis are shown in Table 1. The correlation coefficient between the blast percentage and the Hes1 mRNA level was −0.395, indicating that the elevated Hes1 expression level was independent of the increase in the blast percentage.

To investigate the role of Hes1 in CML blast crisis, we measured the Hes1 mRNA by real-time RT-PCR in 5 human cell lines (K-562,[27] JK-1,[28] KCL-22,[29] TS9:22,[30] and JURL-MK1[31]), which were derived from CML in blast crisis. We found that, in 3 of 5 CML blast crisis cell lines, Hes1 mRNA levels were elevated compared with the normal bone marrow sample (Figure 6B). We transduced a dominant-negative Hes1 (dnHes1) lacking a C-terminal WRPW domain via retrovirus vector into the 3 cell lines (K-562, TS9:22, and JURL-MK1) in which Hes1 mRNA levels were elevated. Indeed, in 2 of these 3 cell lines, proliferation was significantly suppressed by transduction of dnHes1 (Figure 6C). The repression of C/EBP-α by Hes1 was also observed in Hes1-transduced KSLs, CMPs, and GMPs compared with control vector-transduced KSLs, CMPs, and GMPs (Figure 6D). When C/EBP-α retrovirus vector was transduced to Hes1-transduced KSLs, CMPs, and GMPs, all of these cells differentiated to segmented neutrophils, suggesting that the expression of C/EBP-α reversed the function of Hes1 (supplemental Figure 6).

Discussion

In the present study, we demonstrated that retroviral transduction of Hes1 readily immortalizes myeloid progenitors at various stages.

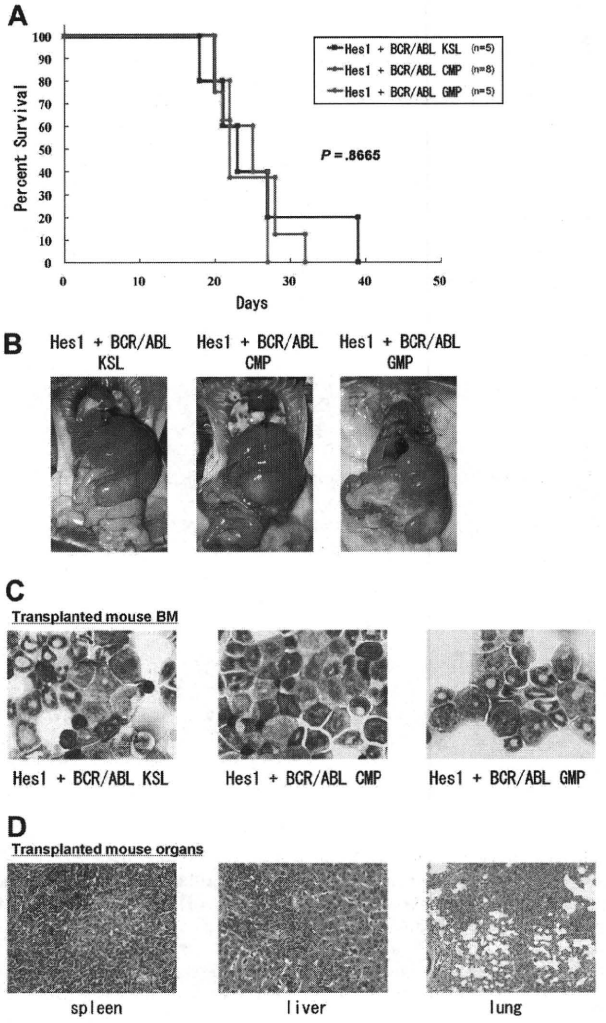

Figure 4. CMPs and GMPs transduced with the combination of Hes1 and BCR-ABL rapidly induced AML/blast crisis of CML. (A) Survival curves of mice. KSLs (n = 5), CMPs (n = 8), and GMPs (n = 5) transduced with the combination of Hes1 and BCR-ABL developed fatal AML/CML in blast crisis-like disease within 18 to 39 days, 20 to 32 days, and 20 to 27 days, respectively. Numbers of injected cells ranged 17×10^2 to 2.6×10^4 for KSLs, 5.5×10^4 to 15×10^4 for CMPs, and 4.0×10^4 to 13.8×10^4 for GMPs. There was no significant difference in latency of penetrance ($P < .867$). Statistical differences were determined using the log-rank test. Three independent experiments were performed, and the total numbers of transplanted mice are shown. (B) Tissue distribution of the leukemic cells. Mice transplanted with KSLs, CMPs, and GMPs transduced with the combination of Hes1 and BCR-ABL invariably demonstrated marked hepatosplenomegaly and lung hemorrhage, both resulting from infiltration of leukemic cells. (C) The morphology of bone marrow cells from representative recipient mice. Increased myeloid blasts were seen with no significant difference among KSLs, CMPs, and GMPs. (D) Histology of spleen, liver, and lungs from representative mice receiving Hes1$^+$BCR-ABL$^+$ GMPs. Vast infiltration of leukemic cells is seen. There were no differences in the histology among mice receiving Hes1$^+$BCR-ABL$^+$ KSLs, CMPs, and GMPs.

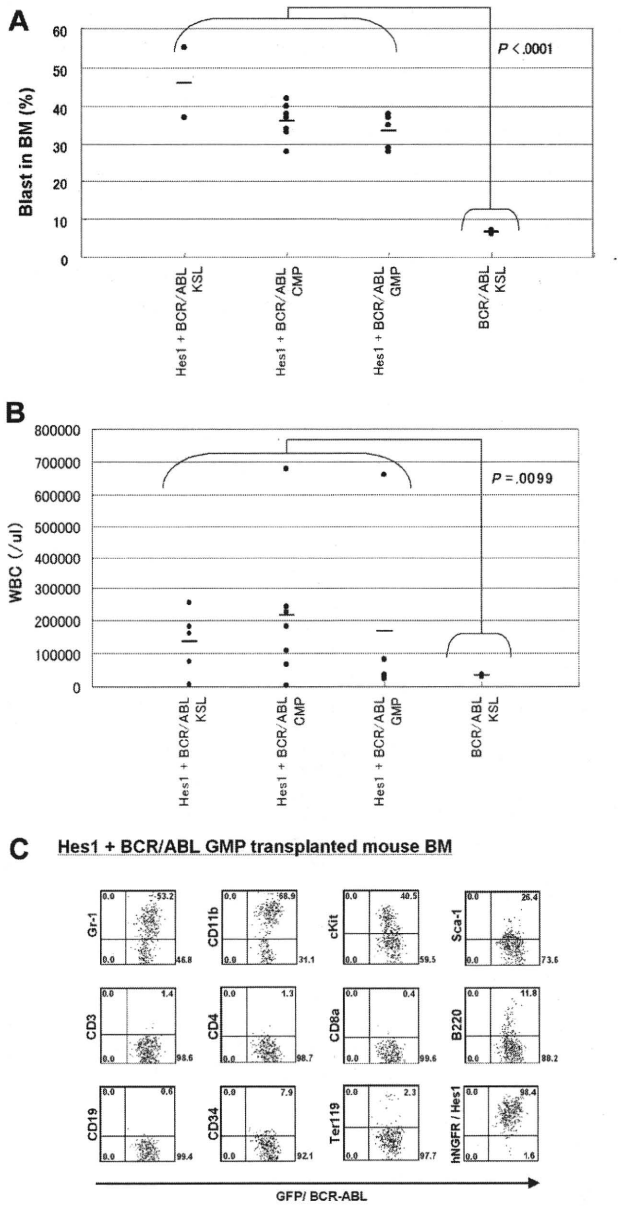

Figure 5. Comparisons of blast percentages in the bone marrow and peripheral blood leukocyte counts between mice receiving KSLs transduced with BCR-ABL alone and those receiving KSLs, CMPs, and GMPs transduced with the combination of Hes1 and BCR-ABL. (A) Blast ratios in the bone marrow. The mean blast ratios in all nucleated bone marrow cells were 6.5% ± 0.7% and 36.5% ± 6.9% in mice receiving KSLs transduced with BCR-ABL alone and in those receiving KSLs, CMPs, and GMPs transduced with the combination of Hes1 and BCR-ABL, respectively. The difference was statistically significant by the 2-sample *t* test with Welch correction ($P < .001$). (B) Peripheral white blood cell counts (WBCs). WBCs were 3.4 ± 0.6 × $10^4/\mu L$ and 17.8 ± 20.3 × $10^4/\mu L$ in mice receiving KSLs transduced with BCR-ABL alone and in those receiving KSLs, CMPs, and GMPs transduced with the combination of Hes1 and BCR-ABL, respectively. The difference was statistically significant by the 2-sample *t* test with Welch correction ($P < .001$). (C) Flow-cytometric analysis of bone marrow cells from mice receiving GMPs transduced with the combination of Hes1 and BCR-ABL. The dot plots represent Gr-1, CD11b, c-Kit, Sca-1, CD3, CD4, CD8a, B220, CD19, CD34, Ter119, and NGFR labeled with the corresponding PE-conjugated monoclonal antibody versus expression of GFP/BCR-ABL. NGFR is a marker of Hes1, and GFP is a marker of BCR-ABL transduction. The bone marrow cells derived from mice receiving KSLs or CMPs transduced with the combination of Hes1 and BCR-ABL showed essentially the same pattern (supplemental Figure 5A-B).

Moreover, when BCR-ABL is transduced together, Hes1 tranforms differentiated myeloid progenitors, such as CMPs and GMPs, in addition to hematopoietic stem cell-rich population, such as KSLs, to AML/CML in blast crisis-like cells, rapidly killing recipient mice. This result is in sharp contrast to the fact that a hematopoietic stem cell-containing population is required for BCR-ABL to cause MPN-like disease.

Hes1 is known as an effector molecule functioning downstream of Notch signaling. The activating mutations of the extracellular heterodimerization domain and/or the C-terminal PEST domain of Notch1 have been identified in approximately 50% of human T-cell acute lymphoblastic leukemias.[10,32] We have recently identified gain-of-function mutations of *Notch2* in conjunction with increased copy numbers of the mutation-carrying *Notch2* allele in a subset of B-cell lymphomas.[11] A possible association between deregulated Notch signaling is also reported in Hodgkin lymphoma, anaplastic large cell lymphoma, small-cell lung cancer, and prostate adenocarcinoma, etc.[33] Regarding myeloid malignancies, however, only one paper reports the identification of the activating mutation of Notch1 in 1 of 12 human AML samples.[34] Given that Notch signaling is among the strongest inducers of T-cell lineage commitment[12,13] and that increased Notch signaling could block myeloid lineage commitment,[15] deregulated Notch signaling might antagonize, rather than promote, the development of myeloid malignancies. However, Hes1 does not necessarily represent Notch signaling. Indeed, other extracellular signaling, such as Sonic Hedgehog,[35] could affect Hes1 expression, and cross-talk between Hes family proteins and molecules in various cell signaling pathways, such as Stat3,[36] has been demonstrated.

We previously reported that Hes1 preserved highly purified hematopoietic stem cells in vitro and contributed to the expansion of transduced hematopoietic stem cells in the recipients' bone marrow,[7] but the effect of Hes1 transduction on myeloid progenitors was not evaluated in detail. We have now found the myeloid progenitor-immortalizing activity of Hes1. In addition, accumulation of KSL- and GMP-like population in Hes1-transduced cells implicates a role for Hes1 in leukemic stem cells. On the other hand, we have also found that the in vitro growth of the Hes1-immortalized cells is dependent on cytokine signaling and that Hes1 alone is insufficient to be fully leukemogenic when overexpressed. The mainstay of the Hes1 effects on myeloid progenitors appears to be blockade of differentiation, although other functions, such as reversion from the quiescent state to the actively cycling state,[21] may also be involved. In the present study, we confirmed that Hes1 expression represses C/EBP-α, a transcription factor having important roles in myeloid differentiation, in mouse KSLs and committed progenitors as we reported.[15] Moreover, transduction of C/EBP-α reversed the differentiation block caused by Hes1 expression, which partially explains the mechanism of blocked myeloid differentiation by Hes1. C/EBP-α is frequently mutated in AML with the normal karyotype.[37-39] In other human AML without C/EBP-α mutations, reduced C/EBP-α expression, possibly through deregulated epigenetic control, is not uncommon and is associated with poor prognosis.[40,41] Furthermore, mice injected with mutated C/EBP-α-transduced bone marrow cells develop myelodysplastic syndrome and AML.[42] Therefore, reduction of C/EBP-α function is highly relevant to the development and/or progression of myeloid malignancies. Hes1, therefore, might be involved in human myeloid malignancies through suppression of C/EBP-α.

Up-regulation of Hes1 is shown in a subset of human rhabdomyosarcomas[21] and medulloblastomas.[43,44] In the present study, we have detected elevated expression of Hes1 in 8 of the 20 samples from CML in blast crisis patients, but not those from CML